# Real-Time Risk Assessment and Management of Pipelines

Research Project Report 3:

***Corrosion Time Considerations, Corroded and Dented-Gouged Capacity Analysis Biases***

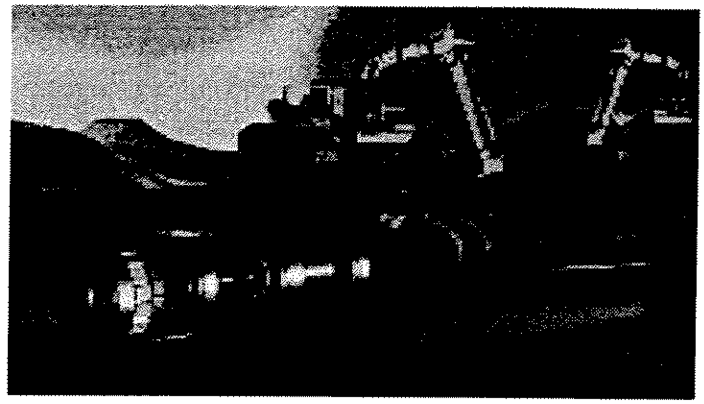

Sponsored by:

***Rosen Engineering***

and

***U.S. Minerals Management Service***


By Professor Robert Bea

***Marine Technology & Management Group***

***Department of Civil and Environmental Engineering***

***University of California at Berkeley***


August 15, 2001

# Real-Time
# Risk Assessment & Management
# of Pipelines

Research Report 3

***Corrosion Time Considerations,***

***Corroded & Dented-Gouged Capacity Analysis Biases***

by

Professor Robert Bea

***Marine Technology & Management Group***

***Department of Civil & Environmental Engineering***

***University of California at Berkeley***

# Table of Contents

# 1 Introduction

Pipeline in-line instrumentation has become a primary means for gathering detailed data on the current condition of the pipeline. It would be very desirable for the pipeline owner, operator, and regulator to have a highly automated process to enable the preliminary assessment of the reliability of the pipeline in its current and project future conditions.

## 1.1 Objective

The objective of the Real-Time RAM Project is to develop, verify, and test procedures that can be used during the in-line instrumentation of pipelines to characterize their reliability.

## 1.2 Project Background

Pipeline in-line instrumentation data can provide a large amount of data on damage and defect (features) in a pipeline. This data must be properly interpreted before the features can be characterized. The detection of features varies as a function of the size and geometry of the features, the in-line instrumentation used, and the characteristics of the pipeline.

Given results from in-line instrumentation, it is desirable to develop an evaluation of the effects of the detected features on the pipeline's integrity. This evaluation requires and analysis of how the detected features might affect the ability of the pipeline to maintain containment.

Evaluation of the effects of uncertainties associated with in-line instrumentation data, pipeline capacity, and operating conditions on a pipeline's abilities to maintain containment can be analyzed using structural reliability methods. During the past five years, the Marine Technology and Management Group at the University of California at Berkeley have been using such methods to evaluate the reliability of pipelines. This work has addressed a variety of types of defects and damage including corrosion, denting, gouging, and cracking. The work has also included development of database structures that can allow storage and use of information gathered from in-line instrumentation in developing improved reliability evaluations for both instrumented and non-instrumented pipelines. One of the products of these studies has been development of a generic framework for the reassessment and requalification of pipelines. This framework involves a three-tiered process that includes qualitative indexing methods (tier 1), simplified reliability based methods (tier 2), and sophisticated probability risk analysis based methods (tier 3). The objective of this approach is to allow pipelines to be reassessed and requalified at the simplest tier possible, utilizing the more advanced tiers only when it is necessary. This project would be focused on development and verification of a tier 2 method.

A parallel project, identified as the Performance of Offshore Pipelines (POP) Project will provide information on the burst pressure capacities on in-place pipelines. The pipelines will be in-line instrumented prior to hydrotesting. The ruptured sections of the pipeline will be retrieved and subjected to laboratory tests. This project will provide data to verify the analytical procedures developed during this project.

## 1.1 Scope of Research

The Real-Time RAM (Risk Assessment and Management) of Pipelines addresses the following key aspects of criteria for in-line instrumentation:

- Development of assessment methods to help manage pipeline integrity to provide acceptable serviceability and safety.
- Definition of reliabilities based on data from in-line instrumentation of pipelines to provide acceptable safety and serviceability.
- Development of assessment processes to evaluate characteristics of in-line instrumented pipelines.
- Evaluation of the effects of uncertainties associated with in-line instrumentation data, pipeline capacity, and operating conditions.
- Formulation of analysis of pipeline reliability characteristics in current and future conditions.
- Validation of the formulations with data from hydrotesting of pipelines and risers provided by the POP (Performance of Offshore Pipelines) Project.
- Definition of database software to collect in-line inspection data and evaluate the reliability of the pipeline.

The first two phases of this project have addressed:

- Development of assessment methods to help manage pipeline integrity to provide acceptable serviceability and safety.
- Definition of reliabilities based on data from in-line instrumentation of pipelines to provide acceptable safety and serviceability.
- Development of assessment processes to evaluate characteristics of in-line instrumented pipelines.
- Formulation of analysis of pipeline reliability characteristics in current conditions.
- Definition of database software to collect in-line inspection data and evaluate the reliability of the pipeline.

These developments have been documented in the first two project reports.

During the current phase of the project, two additional scope topics have been addressed:

- Formulation of analysis of pipeline reliability characteristics in future conditions (time effects), and
- Evaluation of the effects of uncertainties associated with the proposed pipeline capacity evaluation assessments (capacity biases).

The results of the research on these two topics are documented in this report.

## 1.3 Project Tasks

- Develop, verify and test procedures that can characterize the reliability based on the results from in-line instrumentation with various features including corrosion, dents and gouges.
- Evaluate available data from in-line instrumentation including the uncertainties associated with the in-line instrumentation tool itself, and its specification.
- Evaluate the uncertainties associated with in-line inspection data, pipeline demands (operating conditions), and capacities using simplified reliability based methods.
- Develop formulations to analyze reliability of a pipeline in its current condition. The consequence of pipeline failure will be included.

- Develop formulations to determine time-dependent characteristics of pipeline capacities, demands, and uncertainties.
- Develop formulations to determine reliability of pipeline due to time-dependent characteristics of pipeline capacities, demands, and uncertainties.
- The POP Project will be used to verify the analytical procedures developed during this project.
- Summarize comprehensively how to utilize this project into practical operations and service in industry.
- Document the results in four project phase reports.
- Transfer the forgoing results to project sponsors in five project meetings.

Thus, far this project has addressed the following tasks:

- Develop, verify and test procedures that can characterize the reliability based on the results from in-line instrumentation with various features including corrosion, dents and gouges.
- Evaluate available data from in-line instrumentation including the uncertainties associated with the in-line instrumentation tool itself, and its specification.
- Evaluate the uncertainties associated with in-line inspection data, pipeline demands (operating conditions), and capacities using simplified reliability based methods.
- Develop formulations to analyze reliability of a pipeline in its current condition.
- Document the results in two project phase reports.
- Transfer the forgoing results to project sponsors in three project meetings.

During this phase of the project, the following additional tasks have been addressed:

- Formulation of analysis of pipeline reliability characteristics in future conditions (time effects),
- Evaluation of the effects of uncertainties associated with the proposed pipeline capacity evaluation assessments (capacity biases),

- Documentation of the results in a third project phase report.

The results of the work on these two three tasks are documented in this report (Report 3).

# 2 Time Dependent Reliability Analyses

## 2.1 Time Dependent Process: Corrosion

Corrosion is a very complex electro-chemical-mechanical time-dependent process that is a function of what is transported in the pipeline or riser, what surrounds the exterior of the pipeline or riser, and how the corrosion is managed. Both pipeline wall thickness and strength can be diminished. Primary corrosion rate determining parameters include temperature, water composition (pH, salinity), and concentration (collection & stagnation sectors); product composition (chemical composition, pH); operational parameters including flow rates, regime, pressures, and oil-water wetting; steel – weld properties including macro and micro structure, alloying elements, and consumables; sulphate reducing bacterial (SRB) count and types; deposits - coatings on the steel surfaces; steel cracking (stress corrosion fatigue); erosion due to the transport of solids and 'stray' currents associated with electrical operating equipment and, and other metals that can come into or are placed in contact with the pipeline.

Anything that can accelerate the transport of electrons from a cathode to an anode will accelerate corrosion, and vice versa. In general, all of the parameters cited can be expected to change during the life of a pipeline because the sources of oil, water, and gas transported through a pipeline are changing and because the external environmental and operational conditions are continuously changing. Similar statements can be made regarding the effects of changes in space along the length and around the perimeter of the pipeline.

Corrosion management is paramount if corrosion is to be controlled in pipelines and risers. Management processes include cathodic protection, dehydration, inhibition, coatings, use of bactericides, pH neutralizers, inspections, instrumentation, and use of coupons to indicate corrosion rates. Once the steel has been lost and its properties degraded, they can not be restored other than by replacement (liners, sleeves). For long-life pipelines, corrosion management, or lack thereof, can pay dividends.

Petroleos Mexicanos (PEMEX) have developed an extensive database on measured (ultrasonic measurements) corrosion in pipelines and risers in the Bay of Campeche (Lara, et al, 1998). Fig. 1 identifies the locations in which corrosion was measured. The reported corrosion is based on the maximum loss of metal thickness reported at each location along the pipeline. Two locations are of particular interest: Zone E and Zone F. Zone E is at the lower section of the riser. Zone F is in the expansion loop portion of the pipeline. The reported corrosion in these zones is internal.

The pipelines range in diameter from 406 mm to 914 mm. The pipelines generally transport low sulfur oil, gas, and oil and gas that ranges in temperature from 30° C (average water temperature) to 110° C with an average of about 80° C. Bacterial counts are low due to the generally very high temperature products. These pipelines are cathodically protected with sacrificial anodes supplemented with pipeline coatings.

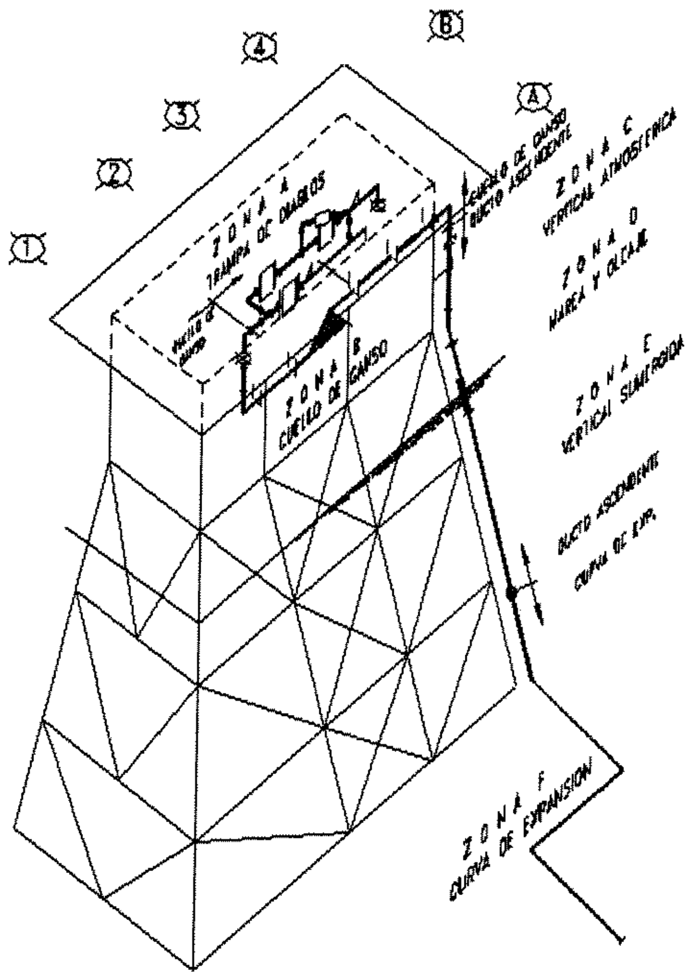


Fig. 1. Zones for corrosion gauging inspections

Fig. 2 summarizes corrosion rate data from all of the pipelines in Zones E and F. The median corrosion rate is 0.015 inches per year for both Zones. The corrosion rate has a Coefficient of Variation of 68 %. Fig. 3 and Fig. 4 summarize data for the oil, and gas service pipelines as a function of their age. The term 'average' refers to the average of the maximum wall thickness loss over a given period of time.

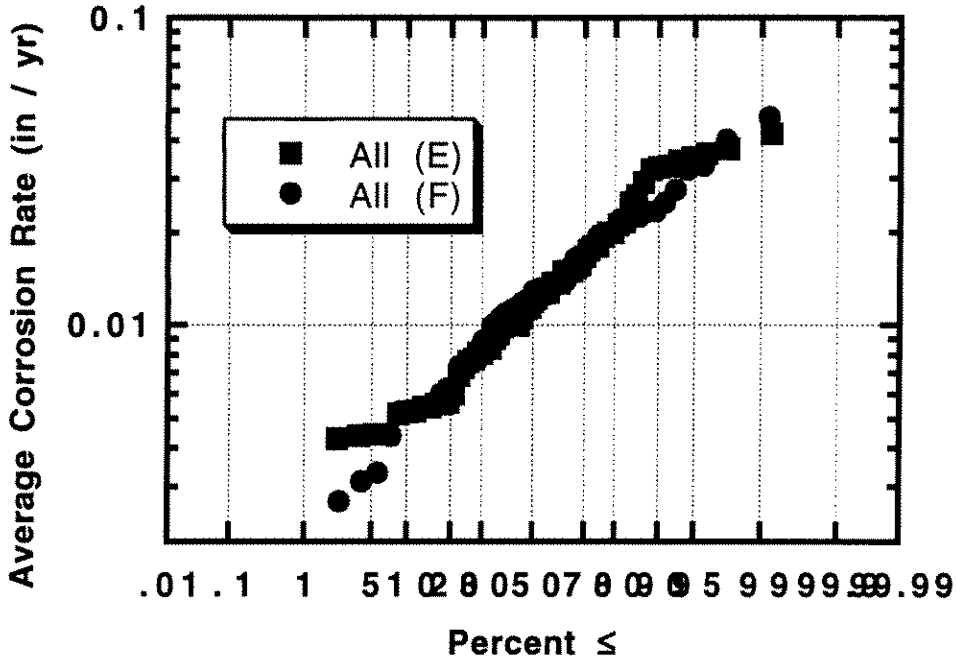


Fig. 2. Corrosion rate data for all pipelines (Lognormal probability scales)

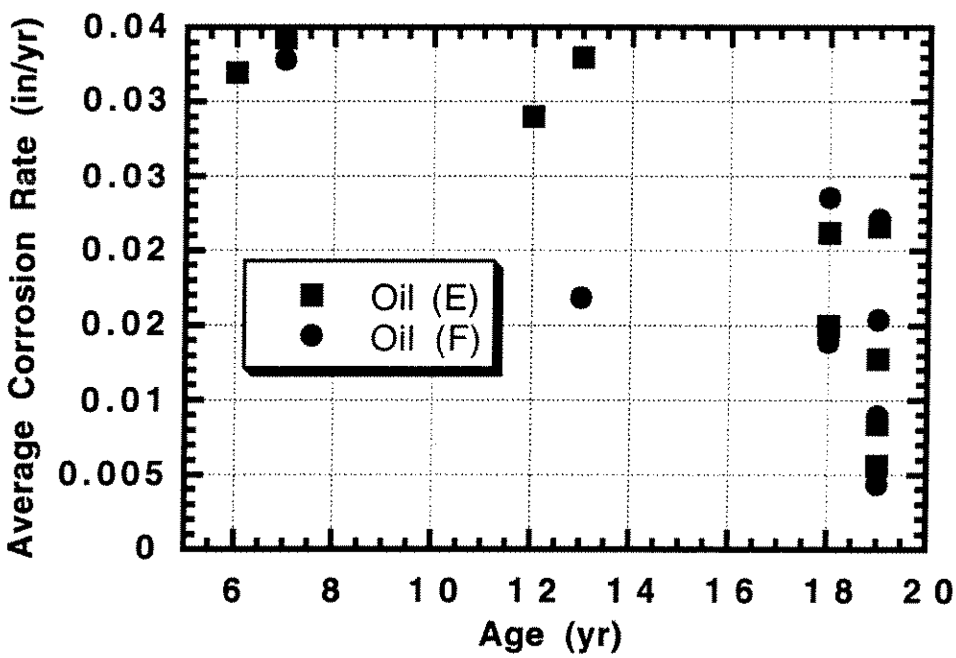


Fig. 3. Oil service corrosion rates as function of pipeline age

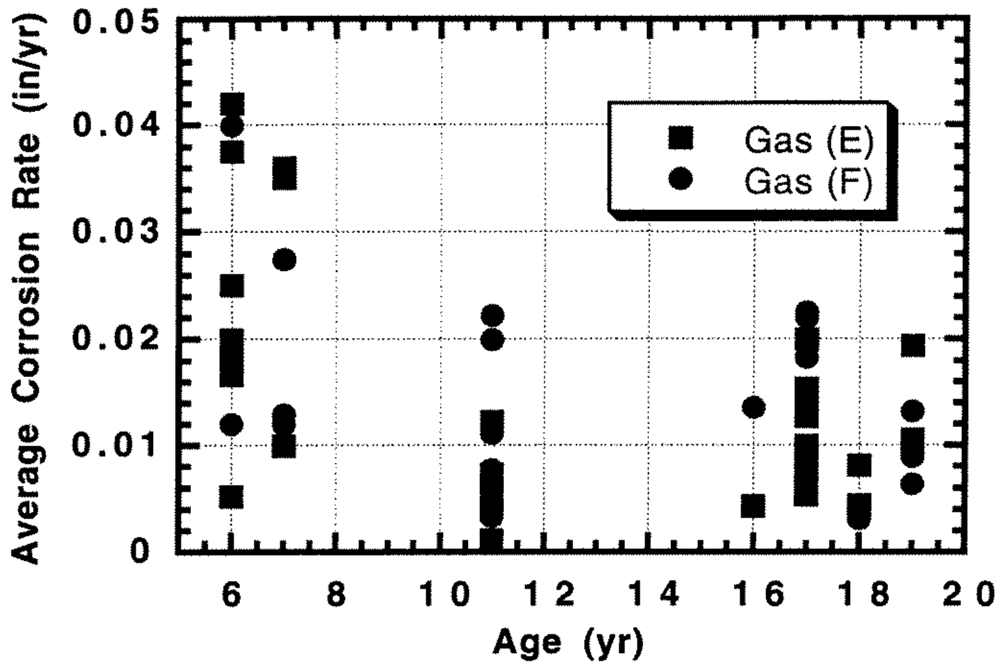


Fig. 4. Gas service corrosion rates as function of pipeline age

There is a definite decrease in the corrosion rates with time for all services. The initial rates of corrosion for gas lines are generally about half those associated with the oil lines. The rate of corrosion is much higher early in the life of the pipeline.

Fig. 5 and Fig. 6 summarize pipeline corrosion rates for pipelines that are 17 to 19 years old. The median rate of corrosion for oil pipelines is 0.015 in / yr (15 mills per yr, mpy). The oil pipelines corrosion rate has a Coefficient of Variation (COV) of 40%. The median rate of corrosion for gas pipelines is 0.010 in/yr (10 mpy). The gas pipelines corrosion rate has a COV of 40%.

This is extremely useful data for the prediction of corrosion rates for this particular population of pipelines. Due to the unique characteristics of the products and environment, the data can not be easily applied to other populations of pipelines.

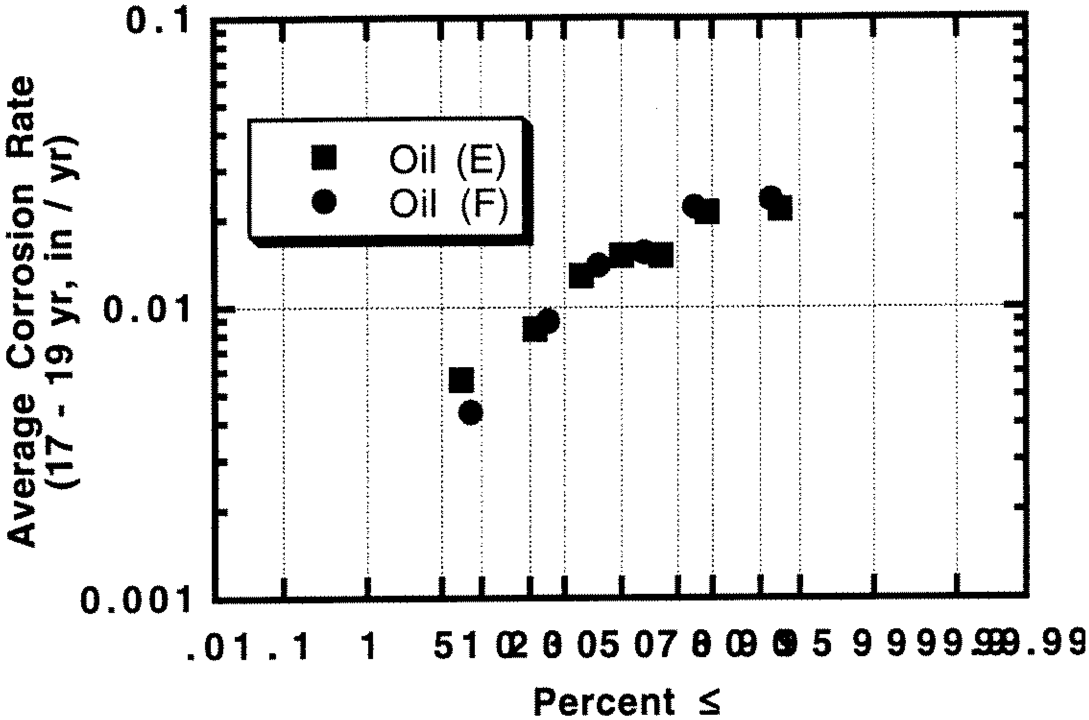


Fig. 5. Oil pipeline corrosion rates for ages 17 – 19 years (Lognormal probability scales)

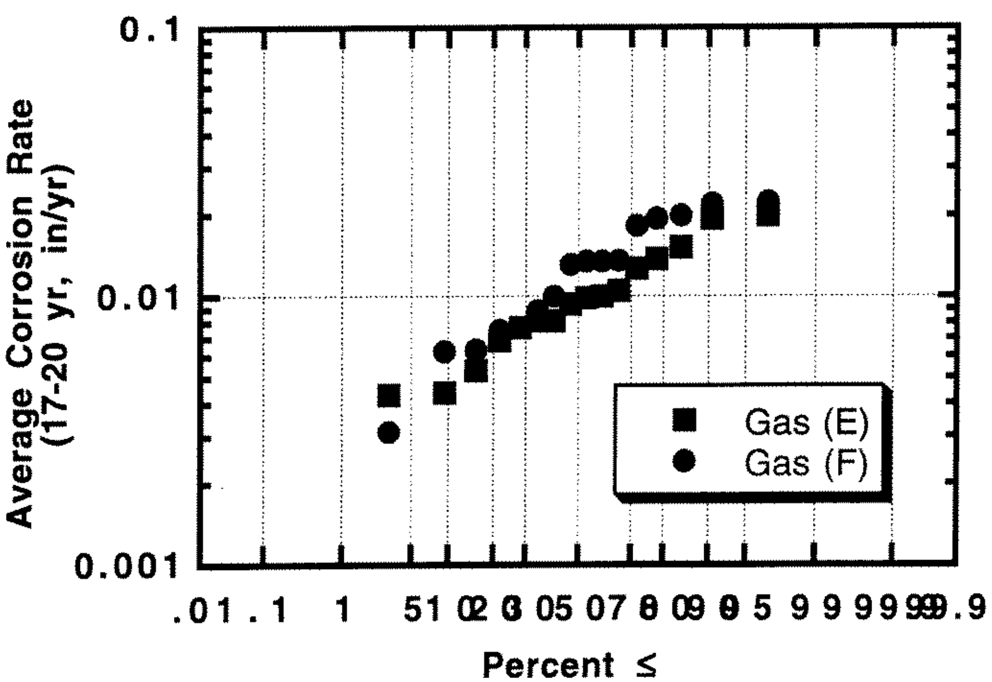


Fig. 6. Gas pipeline corrosion rates for 17 – 19 years (Lognormal probability scales)

## 2.2 Corrosion – Time Dependent Reliability

Pipeline reliability is a time dependent function that is dependent on the corroded thickness of the pipeline ($t_{ci/e}$). The corroded thickness is dependent on the rate of corrosion and the time that the pipeline or riser is exposed to corrosion. This time dependency can be clarified with the following expression for a time dependent Safety Index ($\beta$):

$$\beta = \ln (Kp\ t - Kp\ t_{ci/e}) / \sigma_{lnp/}$$

where:

$$Kp = (2.4\ SMTS / D\ SCF\ Po)$$

Recall that the probability of failure, Pf, is very approximately expressed by:

$$Pf = 10^{-\beta}$$

Po is the median maximum operating pressure. $t_{ci/e}$ is the wall thickness loss due to internal and external corrosion. $\sigma_{lnp/R}$ is the total uncertainty (standard deviation of the logarithms) in the burst pressure capacity and the maximum operating pressure. As developed in the first two project reports, this formulation is based on Lognormally distributed independent burst pressure capacities and peak internal pressures.

If one defines:

$$Kp\ t = FS_{50}$$

where $FS_{50}$ is the median factor of safety in the burst capacity of the pipeline or riser. Then:

$$\beta = \ln (FS_{50} - FS_{50} (t_{ci/e} / t)) / \sigma_{lnp/R}$$

As the pipeline corrodes, the reduction in the pipeline or riser wall thickness leads to a reduction in the median factor of safety that in turn leads to a reduction in the Safety Index (or an increase in the probability of failure). In addition, as the pipeline corrodes, there is an increase in the total uncertainty due to the additional uncertainties associated with the corrosion rates and their effects on the burst capacity of a pipeline or riser.

An analytical model for the increase in total uncertainty as a function of the corrosion can be expressed as:

$$\sigma_{\ln p/R}|t = \sigma_{\ln p/R}|to\ (1 - t_{ci/e} / t)^{-1}$$

where $\sigma_{\ln p/R}|t$ is the uncertainty at any given time, t, $\sigma_{\ln p/R}|to$ is the uncertainty at time t = 0, $t_{ci/e}$ is the corroded thickness and t is the initial thickness. When $t_{ci/e}$ / t = 0.5 the initial uncertainty would be increased by a factor of 2. Results for $\sigma_{\ln p/R}|to$ = 0.2 and = 0.30 and $FS_{50}$ = 2.0 (same as median bias used previously) are summarized in Fig. 7.

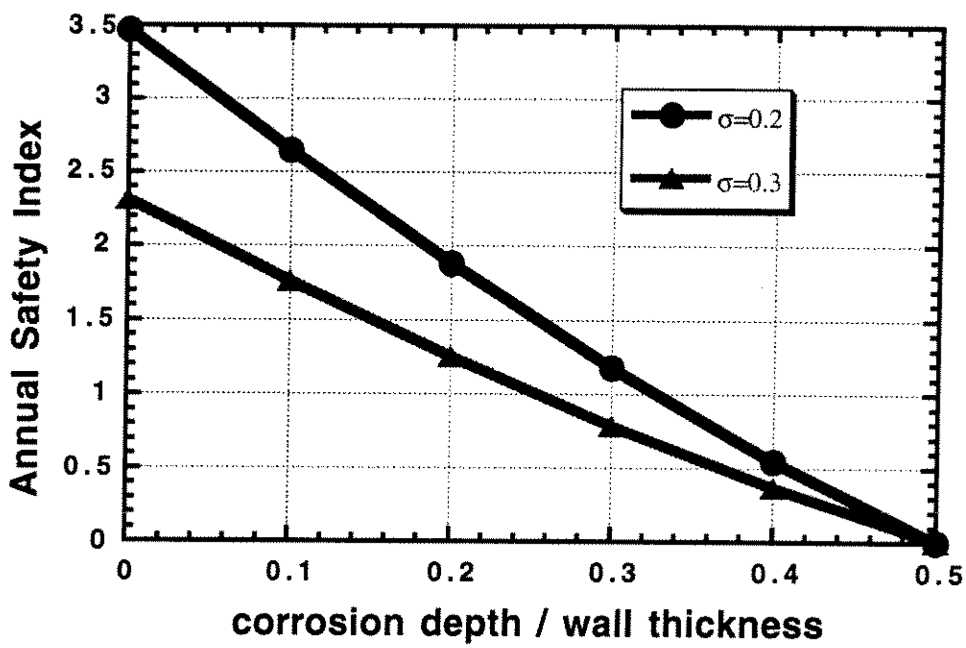


Fig. 7. Influence of corrosion depth and uncertainty on annual Safety Index

Additional insight into the change in the uncertainty associated with the pipeline capacity associated with the loss of wall thickness due to corrosion, can be developed by the following:

$$\bar{t'} = \bar{t} - \bar{d}$$

t' is the wall thickness after the corrosion, t is the wall thickness before corrosion, and d is the maximum depth of the corrosion loss. Bars over the variables indicate mean values.

Based on First Order – Second Moment methods, the standard deviation of the wall thickness after corrosion can be expressed as:

$$\sigma_{t'} = \sqrt{\sigma_t^2 + \sigma_d^2}$$

The Coefficient of Variation (COV = V) can be expressed as:

$$V_{t'} = \frac{\sigma_{t'}}{\bar{t}'} = \frac{\sqrt{(V_t \bar{t})^2 + (V_d \bar{d})^2}}{\bar{t} - \bar{d}}$$

A representative value for the COV of t would be 2%. A representative value for the COV of d would be Vd = 40%.

## 2.3 Example Applications

Fig. 8 summarizes the foregoing developments for a 16-in. ((406 mm) diameter pipeline with an initial wall thickness of t = 0.5 in. (17 mm) that has an average rate of corrosion of 10 mpy (0.010 in. / yr, 0.25 mm / yr). The dashed line shows the results for the uncertainties associated with the wall thickness. The solid line shows the results for the uncertainties that include those of the wall thickness, the prediction of the corrosion burst pressure, and the variabilities in the maximum operating pressure.

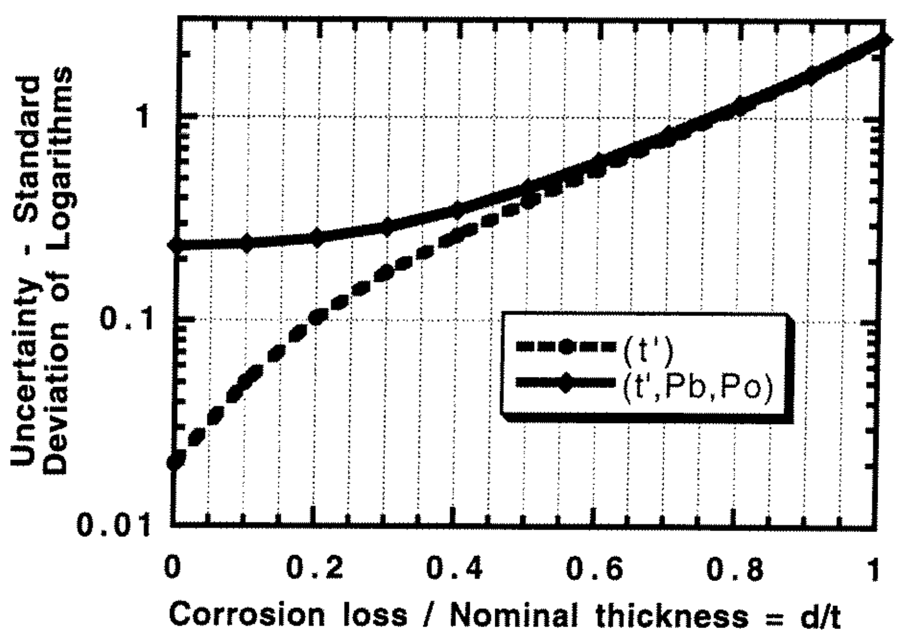


Fig. 8. Uncertainty in pipeline wall thickness and burst pressure capacity as a function of the normalized loss in pipeline wall thickness.

At the time of installation, the pipeline wall thickness COV is equal to 2%. But, as time develops, the uncertainties associated with the wall thickness increase due to the large uncertainties associated with the corrosion rate – maximum depth of corrosion. The solid line that reflects all of the uncertainties converges with the dashed line that represents the uncertainties in the remaining wall thickness, until at a time of about 20 years, the total uncertainty is about the same as that of the remaining wall thickness ($V_{t-d} \approx 25$ %). As more time develops, there is a dramatic increase in the COV associated with the remaining wall thickness. These uncertainties are dominated by the uncertainties attributed to the corrosion processes.

These observations have important ramifications on the probabilities of failure – loss of containment of the pipeline. After the 'life' of the pipeline is exceeded (e.g. 20 to 25 years), one can expect there to be a rapid and dramatic increase in the uncertainties associated with the corrosion processes. In addition, there will be the continued losses in wall thickness. Combined, these two factors will result in a dramatic increase in the probability of failure of a pipeline.

Fig. 9 summarizes example results for a 16-in. (406 mm) diameter, 0.5 in (13 mm) wall thickness pipeline that has a maximum operating pressure (MOP) of 5,000 psi (34.5 Mpa). The COV associated with the MOP is 10 %. The pipeline is operated at the maximum pressure, and at 60 % of the maximum operating pressure for a life of 0 to 50 years. The average corrosion rate was taken as 10 mpy. For the 60 % pressured line, during the first 20 years, the annual probability of failure rises from 1E-7 to 5 E-3. After 20 years, the annual probability of failure rises very quickly to values in the range of 0.1 to 1. Perhaps, this is why the observed pipeline failure rates associated with corrosion in the Gulf of Mexico are in the range of 1 E-3 per year.

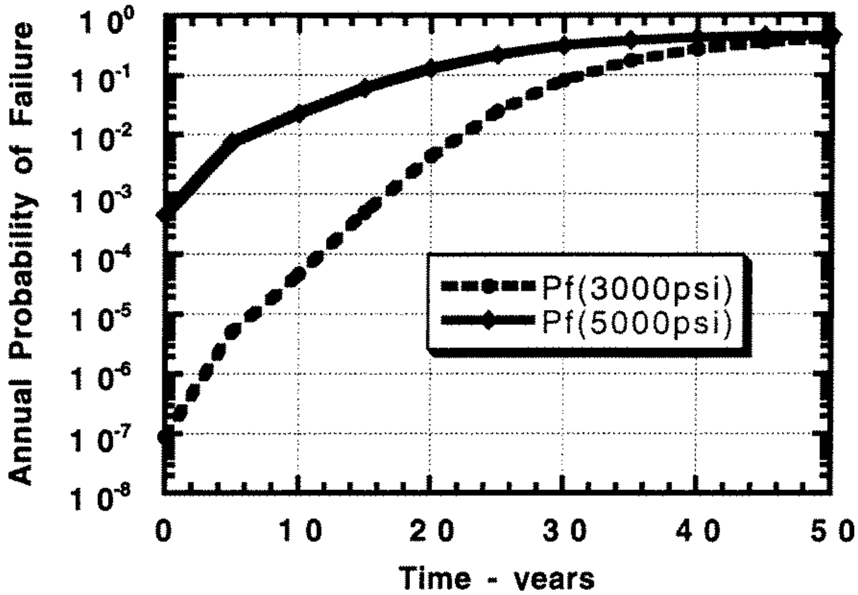


Fig. 9. Example pipeline failure rates as function of exposure to corrosion

Fig. 10 shows the time dependent operating pressures for a 762 mm diameter, 25 mm wall thickness, X60 pipeline that transports crude oil over a distance of 50 km (Collberg, Cramer, Bjornoy, 1996). The operating pressures decrease from a maximum of 3,000 psi (20.7 Mpa, inlet) at the time of commissioning to a maximum of 2,300 psi (15.9 Mpa) at 20 years.

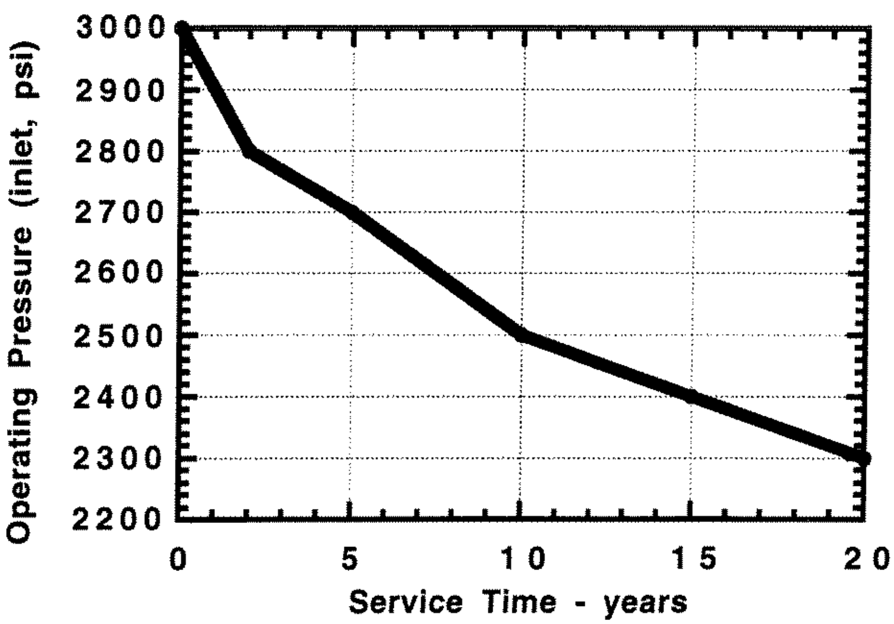


Fig. 10. Example pipeline service time maximum operating pressures

The corrosion in the pipeline is modeled as a time dependent process that is organized into three stages (Fig. 11). The first stage (5 years) is when there is no significant water-cut in the oil stream. The pipeline is effectively protected by the oil wetting of the steel. The best estimate average corrosion rate during Stage 1 is estimated to be 5 mpy. The second stage (10 years) is when there is a significant (above 40 %) water cut in the oil stream. Salt water is in contact with significant portions of the horizontal sections of the pipeline. The best estimate average corrosion rate during this stage is estimated to be 20 mpy. The third stage (5 years) is when there is significant SRB count (above 1E4) due to water flooding of the reservoir with untreated sea water. The best estimate average corrosion rate during this period is estimated to be 50 mpy.

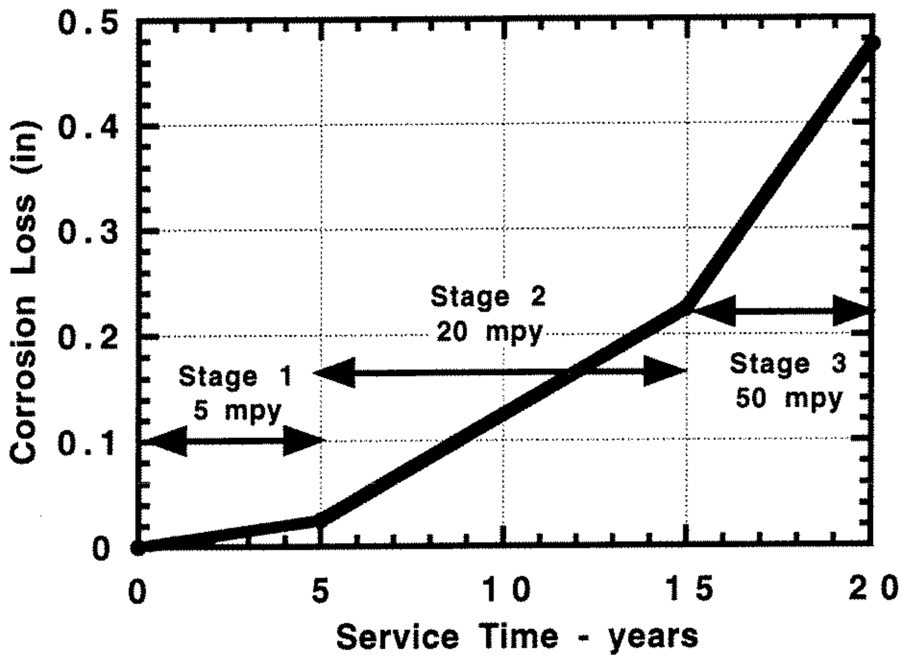


Fig. 11. Example pipeline loss of wall thickness due to corrosion

Fig. 12 summarizes the result of the evaluation of the annual probabilities of loss of containment as a function of the service time. This example recognizes the time changes of the operating pressures (COV = 10 %), corrosion rates, and uncertainties associated with the corrosion losses (COVd = 40 %).

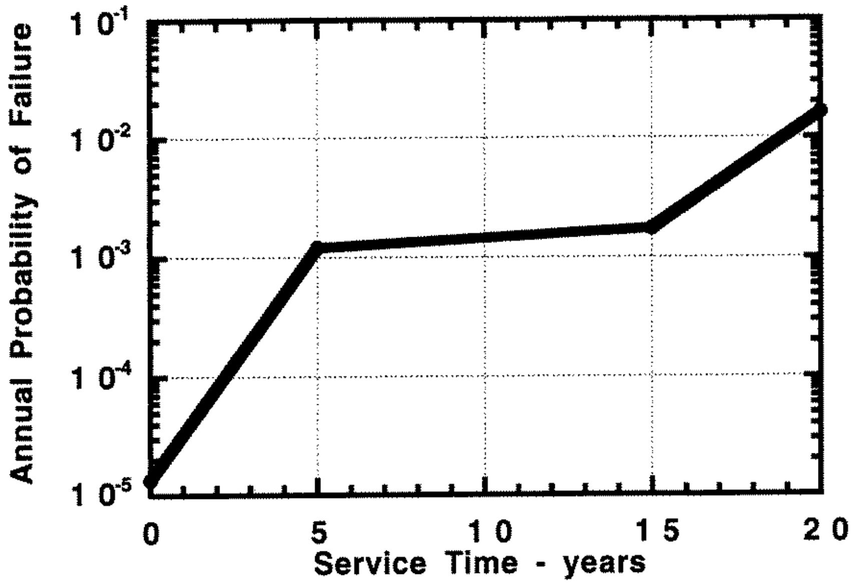


Fig. 12. Example pipeline service time versus annual probability of failure

In Stage 1, there is a relatively rapid rise in the probabilities of failure early in the life of the pipeline due to the increased uncertainties associated with the corrosion damage and the prediction of the burst pressure capacities of the corroded pipeline. In Stage 2, there is a leveling off of the probabilities of failure due to the compensating effects of the lowered operating pressures and the increased corrosion rate and uncertainties associated with the corrosion damage. In Stage 3, there is again a rapid increase in the probabilities of failure due to the large increase in corrosion damage associated with the sulphate reduction bacteria (SRB) effects.

# 3 Bias in Capacity Assessments

## 3.1 Bias Based on Pipeline Test Results

One of the most important parts of a reliability assessment is the evaluation of the 'Bias' that is associated with various ways to determine the capacity of a pipeline. In this development, Bias is defined as the ratio of the true or measured (actual) capacity of a pipeline to the predicted or nominal (e.g. code or guideline based) capacity:

$$\text{Bias} = B_X = \frac{\text{True}}{\text{Predicted}} = \frac{\text{Measured}}{\text{Nominal}}$$

It is important to note that the measured value determined from a laboratory experiment is not necessarily equal to the true or actual value that would be present in the field setting. Laboratory experiments involve 'compromises' that can lead to important differences between the true or actual pipeline capacity and that measured in the laboratory.

One important example of the potential differences between the true pipeline capacity and the experimentally determine pipeline capacity regards laboratory experiments that are used to determine the burst pressure capacity of corroded pipelines. To facilitate the laboratory experiments (controlled parameter variations), the corroded features frequently are machined into the pipeline specimen. This machining process can lead to important differences between actual corroded features and those machined into the specimens; stress concentrations can be very different and residual stresses imparted by the machining process can be very different. In addition, the end caps placed on small specimens can lead to significant longitudinal tensile stresses in the specimen that may not be present in the field conditions. Thus, laboratory results must be carefully regarded and it must be understood that such experiments can themselves introduce Bias into the assessment of pipeline reliability.

Another important example regards true or 'measured' results that are based on results from analytical models. Such an approach has been used to generate 'data' used in several recent major reliability based code and guideline developments. The general approach is to use a few high quality physical laboratory tests to validate or calibrate the analytical model. Then the analytical model is used to generate results with the model's parameters being varied to develop experimental data. One colleague has called "these visual experiments." The primary problems with this approach concern how the model's parameters are varied (e.g. recognition of parameter correlations recognized and definition of the parametric ranges), and the abilities of the model to incorporate all of the important physical aspects (e.g. residual stresses, material nonlinearity). The use of analytical models introduces additional uncertainties and these additional uncertainties should not be omitted. In one recent case, the analytical models have been calibrated based on machined pipeline test sample results. Thus, the analytical models have 'carried over' the inherent Bias incorporated into the physical laboratory tests.

In this study, a differentiation has been made between physical laboratory test data and analytical test data. Further, differentiation has been made between physical laboratory test data on specimens from the field and those that are machined or involve simulated damage and defects. Earlier studies performed on these databases have clearly indicated potentially important differences between physical and analytical test data based Biases and differences between 'natural' and simulated defects and damage.

## 3.2 Bias in Burst Capacities of Corroded Pipelines

The formulations developed during this study to assess the burst capacities of pipelines subjected to general corrosion are:

$$Pbd = 2.0\ t\ SMTS\ /\ (D - t)\ SCF$$

$$Pbd = 2.4\ t\ SMTS\ /\ (D - t)\ SCF$$

$$SCF = 1 + 2\ (d\ /\ R)0.5$$

where Pbd is the burst pressure capacity of the corroded pipeline, t is the nominal wall thickness (including the corrosion allowance), D is the pipeline outside diameter, SMTS is the specified minimum tensile strength (- 3 $\sigma$), and SCF is a stress concentration factor that is due to the corrosion features. The SCF is a function of the depth of corrosion, d ($d \leq t$), and the pipeline radius, R. This formulation was chosen because study of the failure mechanisms associated with burst of naturally corroded mild steel pipelines (corroded over more than 10% of the circumference) indicated that it was the corrosion feature induced local stress increase that was controlling the rupture of the pipeline wall (ductile tearing mode of failure). The SCF (maximum hoop stress / nominal hoop stress) that is due to a notch of depth d in the pipeline cross section that has a radius R. Note that this formulation does not explicitly incorporate the area (length, width) of the pipeline that is corroded. The hoop stress coefficient of 2.0 is multiplied by 1.2 to develop an unbiased estimate of the median transverse ultimate tensile strength of the pipeline steel.

A test database consisting of 151 burst pressure tests on corroded pipelines was assembled from tests performed by the American Gas Association, NOVA, British Gas, and the University of Waterloo (Appendix A). The Pipeline Research Committee of the American Gas Association published a report on the research to reduce the excessive conservatism of the B31G criterion (Kiefner, et al, 1989). Eighty six (86) test data were included in the AGA test data. The first 47 tests were used to develop the B31G criterion, and were full scale tests conducted at Battelle Memorial Institute. The rest of the 86 tests were also full scale and were tests on pipe sections removed from service and containing real corrosion.

Two series of burst tests of large diameter pipelines were conducted by NOVA during 1986 and 1988 to investigate the applicability of the B31G criterion to long longitudinal corrosion defects and long spiral corrosion defects. These pipes were made of grade 414 (X60) steel with an outside diameter of 4064 mm and a wall thickness of 50.8 mm. Longitudinal and spiral corrosion defects were simulated with machined grooves on the outside of the pipe. The first series of tests, a total of 13 pipes, were burst. The simulated corrosion defects were 203 mm wide and 20.3 mm deep producing a width to thickness ratio (W/t) of 4 and a depth to thickness ratio (d/t) of 0.4. Various lengths and orientations of the grooves were studied. Angles of 20, 30, 45 and 90 degrees from the circumferential direction, referred to as the spiral angle, were used. In some tests, two adjacent grooves were used to indicate interaction effects. The second series of tests, a total of seven pipes, were burst. The defect geometries tested were longitudinal defects, circumferential defects, and corrosion patches of varying W/t and d/t. A corrosion patch refers to a region where the corrosion covers a relatively large area of pipe and the longitudinal and circumferential dimensions were comparable. In some of the pipes, two defects of different sizes were introduced and kept far enough apart to eliminate any interaction.

Hopkins and Jones (1992) conducted five vessel burst tests and four pipe ring tests. The pipe diameter were 508 mm. The wall thickness was 102 mm. The pipe was made of X52. The defect depth was 40% of the wall thickness. Jones et al (1992) also conducted nine pressurized ring tests. Seven of the nine were machined internally over 20% of the circumference, the reduced wall thickness simulating smooth corrosion. All specimens were cut from a single pipe of Grade API 5L X60 with the diameter of 914 mm and wall thickness of 22 mm.

As part of a research project performed at the University of Waterloo, 13 burst tests of pipes containing internal corrosion pits were reported by Chouchaoui, et al (1992). In addition, Chouchaoui et al reported the 8 burst tests of pipes containing circumferentially aligned pits and the 8 burst tests of pipes containing longitudinally aligned pits.

The database was analyzed to determine the statistics of the Bias where the Bias is the ratio of the test burst pressure (rupture of the pipe wall) divided by the predicted (analytical) burst pressure. Analysis of the test data based on Eq. 1 (Fig. 13) indicated a median Bias of 1.2 and a Coefficient of Variation (COV) of the Bias of 22 %. Analysis of the test data based on Eq. 2 indicated a median Bias of 1.0 and a COV of the Bias of 22 %. The 1.2 factor was found to be the ratio of the expected ultimate tensile strength to the nominal tensile strength.

Fig. 14 summarizes the test database in the form of the measured burst pressure for the corroded condition divided by the burst pressure for no corrosion (Pbm / Pbo) versus the corrosion depth divided by the nominal wall thickness of the pipeline specimens (d/t). There is a large scatter in the Pbm / Pbo for larger values of d/t. Note that even at values of $d/t \geq 0.7$, the pipeline can sustain as much as 80% of the uncorroded burst pressure (and as low as 40%).

The DNV (2000) and the B31G (effective area) (ASME, 1993) formulations to determine the burst pressures of corroded pipelines include parameters to define the area (length, width, plan geometry) characteristics of the corrosion features. The formulation developed during this study does not include explicit parameters to define the area characteristics of the corrosion features. The 151 physical test database was analyzed to determine if there were definitive trends in the burst pressures that depended on the corrosion area characteristics. The test burst pressures are normalized by the hoop stress at the specified minimum tensile strength (SMTS). The results are summarized in Fig. 15, Fig. 16, and Fig. 17 for the corrosion area defined in terms of its length, its area (length times width), and the term included in the DNV and B31G formulations (square root of the square of the length of the corrosion feature divided by the pipe diameter times the wall thickness), respectively. No definitive trends in the test burst pressures with the corrosion area characteristics were found.

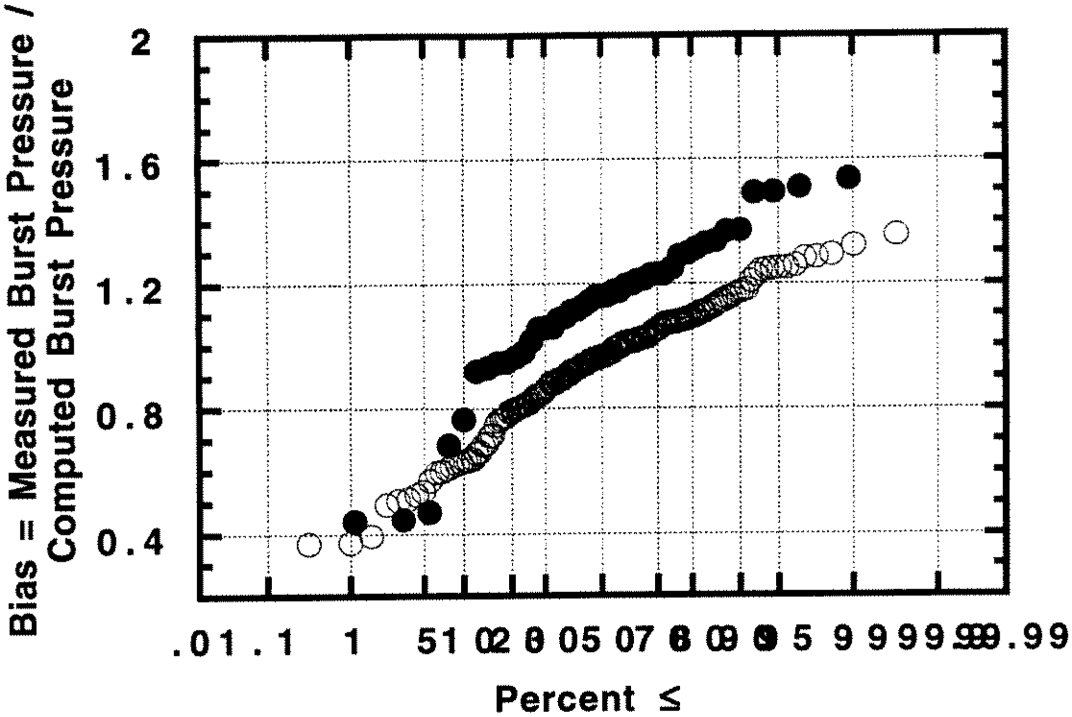


Fig. 13. Bias in design formulations based on SMTS

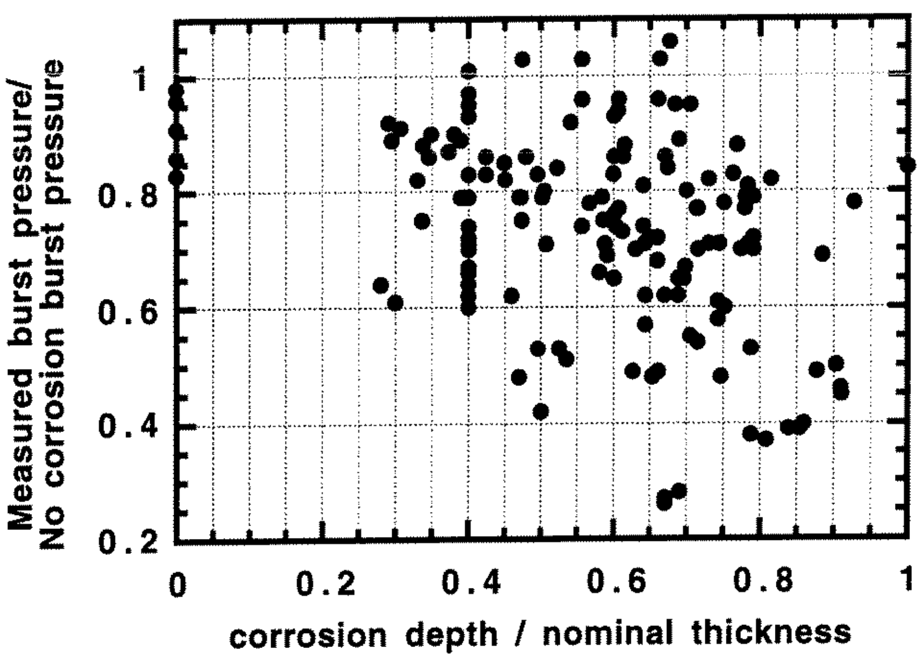


Fig. 14. Variation in burst pressure ratio with d/t

To investigate this finding farther, the DNV (1999), B31G (1993), and Eq. 2 (identified as RAM PIPE) formulations were used to determine the burst pressure bias (measured burst pressure divided by predicted burst pressure). The results for the 151 physical tests are summarized in Fig. 18 and Fig. 19. These tests included specimens that had corrosion depth to thickness ratios in the range of 0 to 1 (Fig. 18). The statistical results from the data summarized in Fig. 18 are summarized in Table 1. The formulation developed during this study has the median bias closest to unity and the lowest COV of the bias. The DNV 99 formulation has a lower bias than B31G, but the COV of the Bias is about the same as for B31 G. The B31G mean Bias and COV in Table 1 compares with values of 1.74 and 54 %, respectively, found by Bai, et al (1997). The burst pressure test data were reanalyzed to include only those tests for d/t = 0.3 to 0.8. The bias statistics were relatively insensitive to this partitioning of the data.

A last step in the analysis of the physical test database was to analyze the Bias statistics based on only naturally corroded specimens (40 of 151 tests). The results are summarized in Fig. 20 and Table 2. The Bias statistics for the DNV 99 and B31G formulations were affected substantially. The results indicate that the machined specimens develop lower burst pressures than their naturally corroded counterparts. Results from other studies indicate that the lower burst pressures for machined specimens are likely due to two factors. The first factor is the stress concentrations associated with machined specimens contrasted with those associated with naturally corroded features. Even though the feature depth and area might be the same for machined and natural features, the local geometry reflected in the shape of the feature has an effect on the local stresses. The second factor are the residual stresses that are developed in the machined specimens. Naturally corroded features do not have such residual stresses.

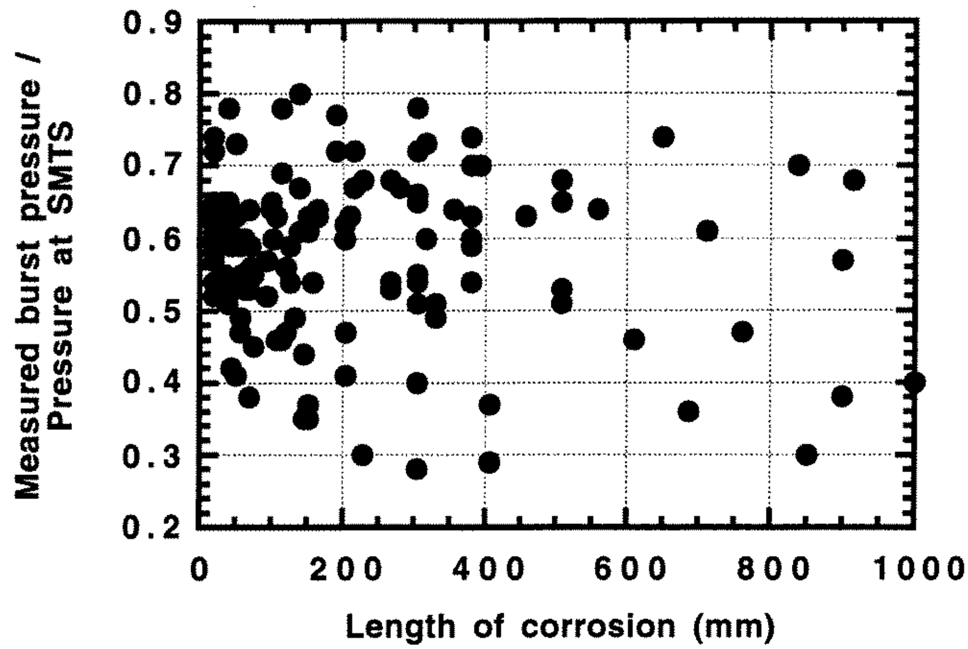


Fig. 15. Pipeline test burst pressures as function of length of corrosion

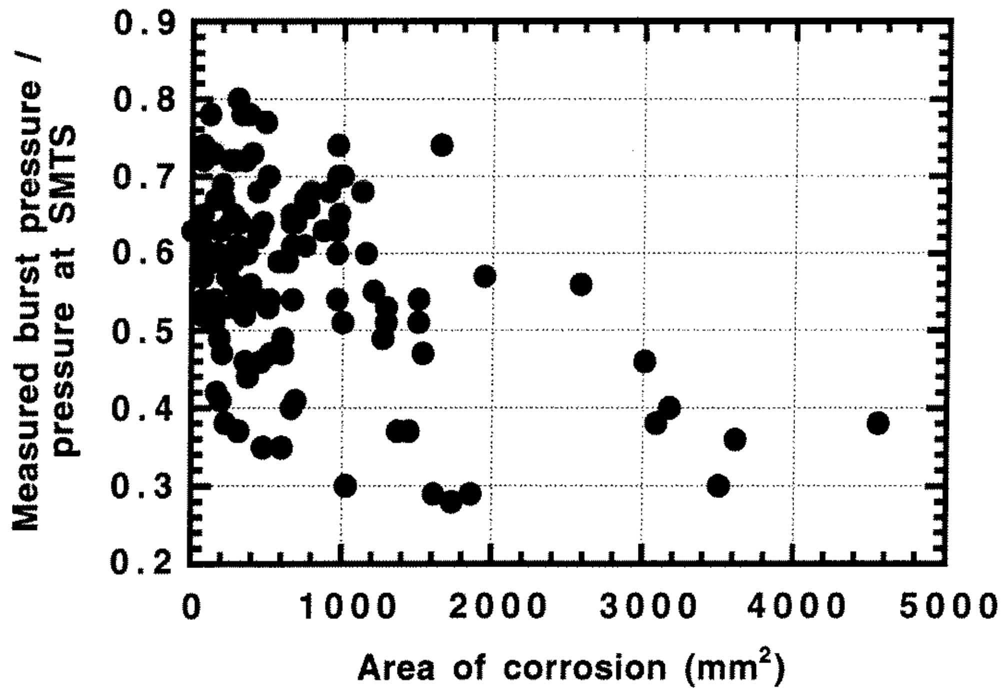


Fig. 16. Pipeline test burst pressures as function of area of corrosion

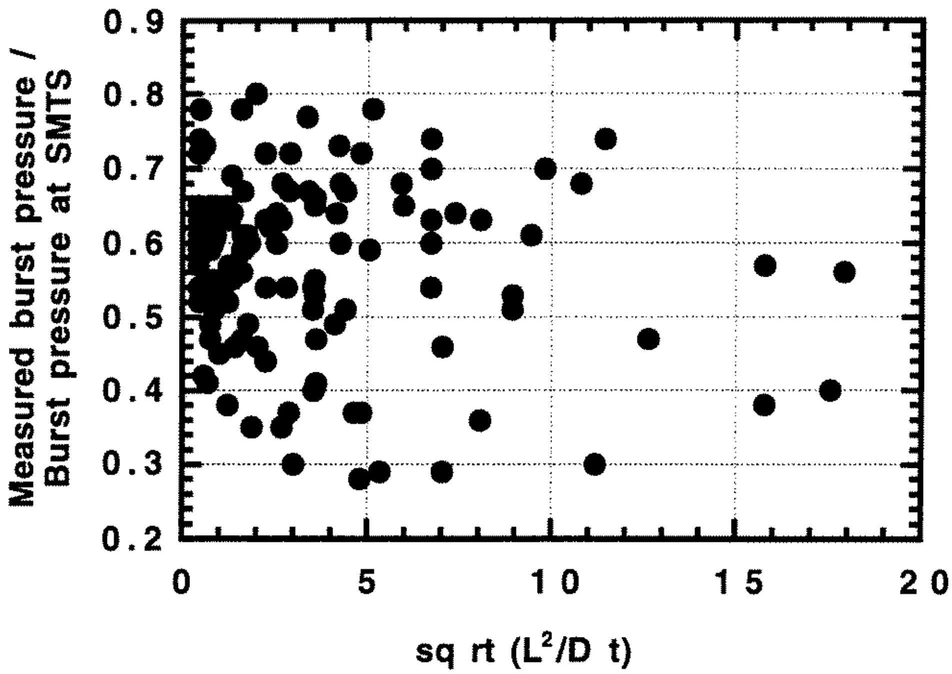


Fig. 17. Pipeline test burst pressures as function of corrosion area parameter

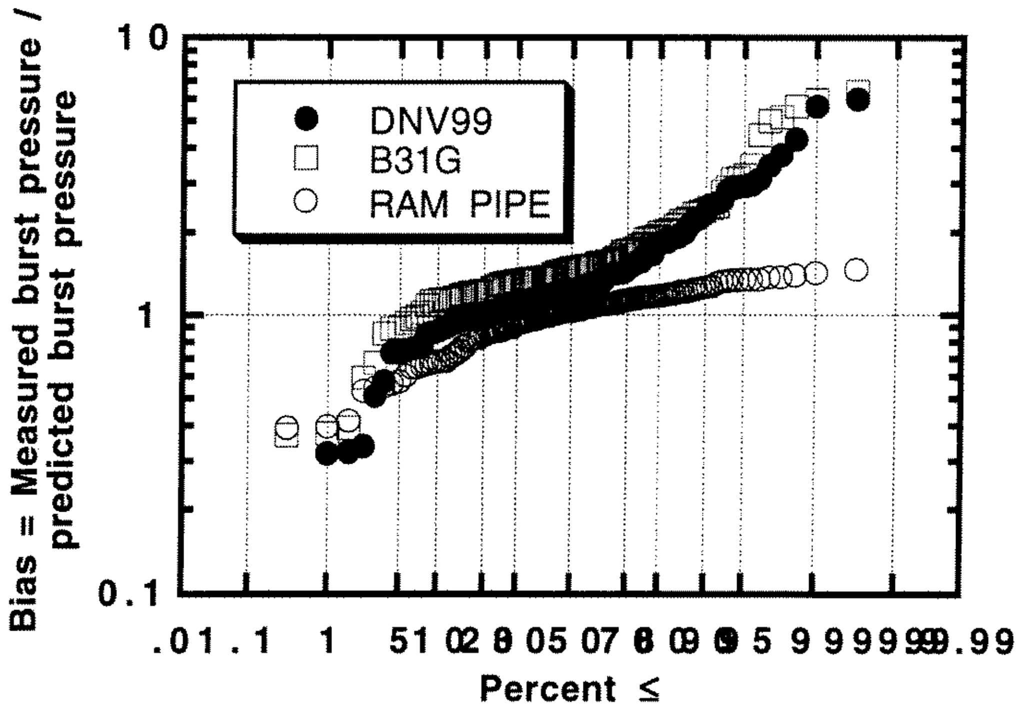


Fig. 18. Bias in burst pressure formulations (Lognormal probability scales)

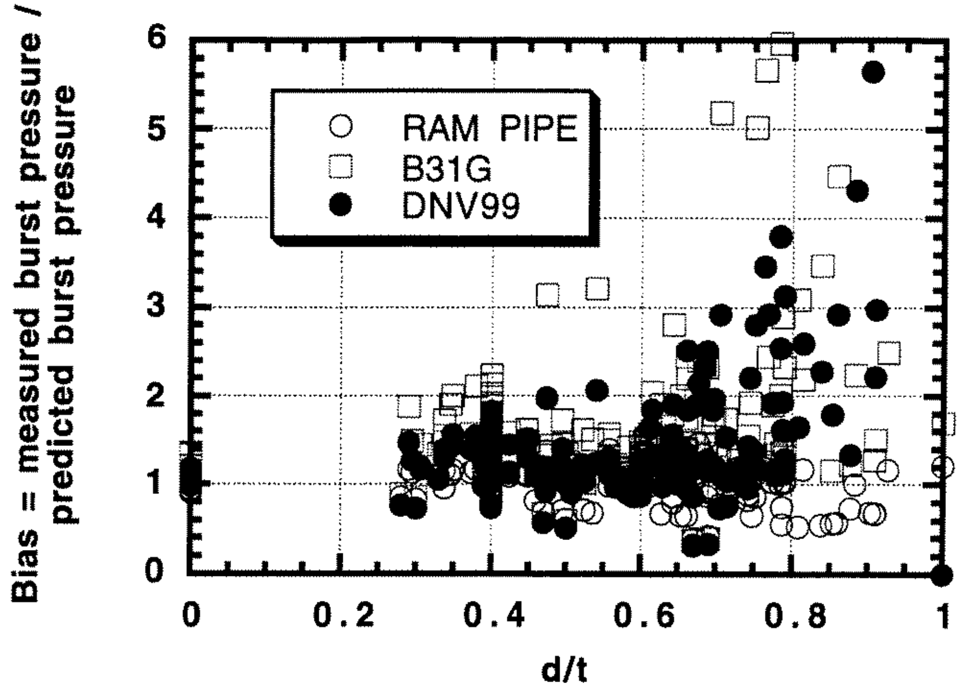


Fig. 19. Bias in burst pressure formulations as function of corrosion depth to wall thickness ratio (d/t)

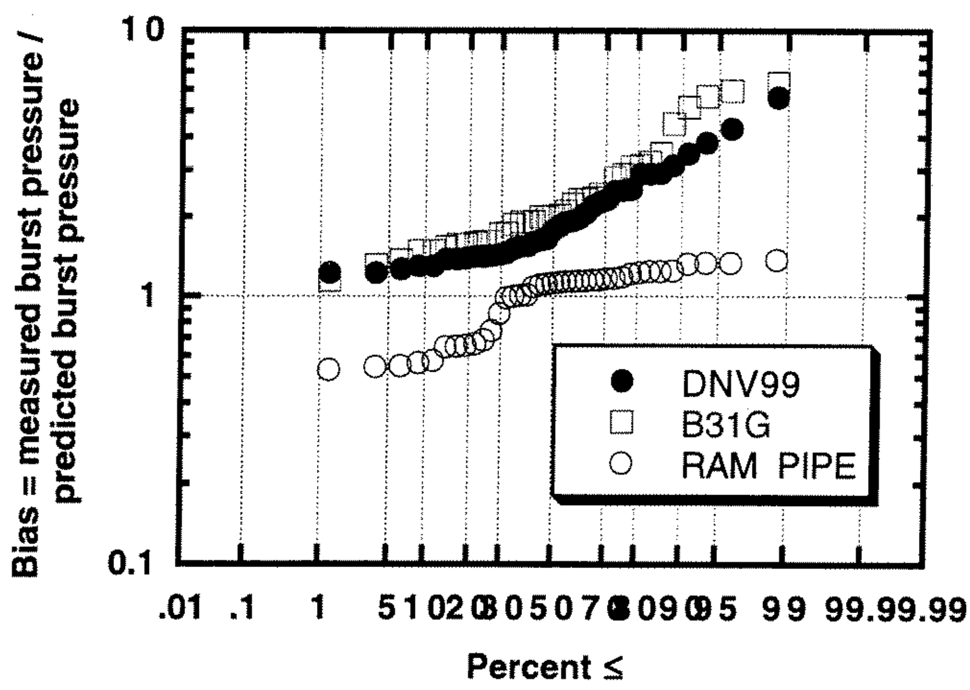


Fig. 20. Bias in burst pressure formulations for naturally corroded test specimens (Lognormal probability scales)

Table 1. Summary of Bias statistics for three burst pressure formulations ($d/t = 0$ to 1)

| Formulation | B mean | $B_{50}$ | $V_B$ % |
|---|---|---|---|
| DNV 99 | 1.46 | 1.22 | 56 |
| B 31 G | 1.71 | 1.48 | 54 |
| RAM PIPE | 1.01 | 1.03 | 22 |

Table 2. Summary of Bias statistics for three burst pressure formulations – naturally corroded tests

| Formulation | B mean | $B_{50}$ | $V_B$ % |
|---|---|---|---|
| DNV 99 | 2.10 | 1..83 | 46 |
| B 31 G | 2.51 | 2.01 | 52 |
| RAM PIPE | 1.00 | 1.10 | 26 |

# 4 Burst Pressure Dented / Gouged Pipelines

Denting is a damage state in that it represents plastic deformation of a pipeline. Denting typically results from highly localized reaction loads that can occur during installation or as a result of outside 'third-party' induced loads during service (e.g. dropped objects or anchor dragging). When the local stresses induced by such loads exceed yield strength, a dent results, permanently deforming the pipe.

## 4.1 Background

A number of research projects in the past 30 years have addressed the strength of pipelines containing various types of defects, including dents (e.g. Kiefner et al, 1973). Three general types of defects have been investigated to evaluate their impact on pipeline integrity: stress concentrations, plain dents, and combination of the two. This classification was developed according to the behavior of the defects under internal pressure.

Stress concentrations consists of V-notches, weld cracks, stress-corrosion cracks, and gouges in pipe that have not been dented. The distinguishing characteristic of this type of defect is that they reduce the pipe wall thickness without changing the curvature of the pipe wall. Considerable research has been conducted into the behavior of this type of defect, and formations are available to predict the severity of reduction in normal burst strength of pipe caused by the presence of this type of defect.

Plain dents are distinguished by a change in curvature of the pipe wall without any reduction in the pipe wall thickness. The behavior of this type of defect has been extensively investigated.

The third defect type represents a combination of the first two and is a dent with a stress concentration. This type of defect represents a type of mechanical damage that is one of the leading causes of leaks and failures in gas distribution and transmission pipelines (Driver, Zimmerman, 1998; Zimmerman, et al, 1998).

### 4.1.1 Plain Dent

Research on the severity and behavior of plain dents in line pipe is summarized in a Pipeline Research Committee report (Eiber, et al 1981). The report reviews and discusses results of conducting capped end pipe burst tests over a range of temperatures (-24 to 90F) on 44 dents. The majority of the dents were placed in the body of the pipe away from longitudinal welds. In all of these tests involving dents remote from the longitudinal weld, the pipes failed at their ultimate strengths and the fractures were at points remote from the dent locations. No effect of temperature was noted in the experimental results.

The results of strain gage readings taken during pressurization of the dents indicated that the principal effect of plain dents is to introduce high localized longitudinal and circumferential bending stresses in the pipe wall. These add to the nominal pressure stresses at some locations in the dent and subtract from them at other locations. Thus, yielding occurs at local locations in the dent at much lower pressure levels than it occurs in the remainder of the pipe body. Without sharp stress concentrations, however, yielding occurs over large enough areas that the pipe has sufficient ductility to yield and accept the plastic flow without failure.

It was found that when dents occur near or on the longitudinal weld, failures can result at low pressures because of cracks that develop in or adjacent to the welds. The cracks probably develop because of the stress concentration associated with weld, and because the various weld zone may exhibit less ductility than the base metal. It was concluded that dents that disturb the curvature of the longitudinal and/or circumferential weld are potentially hazardous defects as they may contain cracks.

The final conclusion of this study is that plain dents whose depth is up to 8 percent of the pipe diameter do not decrease the burst pressure of the section of line pipe. Hence plain dents without stress concentrations represent damage in that the pipe has been plastically deformed but they do not represent an ultimate limit state. This conclusion has also been substantiated by the related work of Belonos and Ryan (1958) on continuous dents.

### 4.1.2 Gouge-in-Dent

Recent research has focused on assessing the severity of mechanical damage defects and the effect of fracture toughness in resisting the failure of these defect types. The conclusion of this research is that fracture toughness does play a significant role in the failure pressure of mechanical damage (gouge-in-dent) defects. Nearly all research on this subject has been conducted at two laboratories; Battelle (e.g. Eiber, et al, 1981; Stephens, et al, 1991), and British Gas Corporation research facilities (e.g. Shannon, 1974; Jones 1981; Hopkins, et al, 1989; Hopkins, 1990). British Gas conducted most of their research using ring cut from pipe, damaged, and then tested on a ring yield-test-machine, using the same type of ring tester used by pipe mills to determine pipe yield strength. British Gas also conducted tests on pipe that was damaged while not pressurized and later on pipe that was pressurized and then damaged.

Battelle's efforts involved testing both pipes that were damaged and then pressurized to failure and pipes damaged while pressurized. It is believed that gouge length is a strong influencing parameter, and it is not possible to use gouge length as a variable in the ring test method.

The research is handicapped by the large number of variables that affect the failure pressure of the damaged pipe. Variables examined to date are gouge depth, gouge length, dent depth, pipe size, pipe toughness, and pipe yield strength. Other variables that are known to affect dent and gouge severity and consequently pipe failure pressure are coatings and the shape and size of the gouging agent. Both hard and soft coatings reduce the amount of gouging but appear to do so in different ways. The softer coatings appear to act as lubricants, allowing the tool to glide over the pipe surface, causing more indentation and less gouging. Tougher coatings are more easily gouged, but in turn protect the pipe underneath, which is gouged less. If the tool is sharp and small, it will gouge more (dent less) than if it is wide and blunt. Real damage done in service is random. Damage can be positioned at any orientation relative to the pipe. Damage also varies depending on the type of equipment being used and the persistence of the equipment operator. It would be impractical to investigate all these variables independently.

## 4.2 Test Data

A database on dented and gouged pipeline tests was assembled (Appendix B, Table 3) based on data published in the foregoing references. This database was organized by the sequence of denting and gouging and type of test performed. Study of this test data indicated the following conclusions:

- Plain denting with smooth shoulders has no significant effect on burst pressures. Smooth shoulder denting is not accompanied by macro or microcracking and the dent is re-formed under increasing internal pressures.

- Denting with sharp shoulders can cause macro and micro cracking which can have some effects on burst pressures and on fatigue life (if there are significant sources of cyclic pressures – straining (Hopkins, 1990). The degree of macro and micro cracking will be a function of the depth of gouging. Generally, given pressure formed gouging, there will be distortion of the metal and cracking below the primary gouge that is about one half of the depth of the primary gouge.

- Gouging can cause macro and micro cracking in addition to the visible gouging and these can have significant effects on burst pressures. In laboratory tests, frequently gouging has been simulated by cutting grooves in the pipe. These grooves can be expected to have less macro and micro cracking beneath the test gouge feature.

- The combination of gouging and denting can have very significant effects on burst pressures and on fatigue life.

- The effects of combined gouging and denting is very dependent on the history of how the gouging and denting have been developed. Different combinations have been used in developing laboratory data. In some cases, the pipe is gouged, dented, and pressured to failure. In other cases, the pipe is dented and gouged simultaneously, and then pressured to failure. In a few cases, the pipe is gouged, pressured, and then dented until the pipeline looses containment. These different histories of denting and gouging have important effects on the propagation of macro and micro cracks developed during the gouging and denting. It will be very difficult for a single formulation to be able to adequately address all of the possible combinations of histories and types of gouging and denting.

- Gouging is normally accompanied by denting a pipeline under pressure. If the pipeline does not loose containment, the reassessment issue is one of determining what the reliability of the pipeline segment is given the observed denting and gouging. Addressing this problem requires an understanding of how the pipeline would be expected to perform under increasing pressure demands (loss of containment due to pressure) or under continuing cyclic strains (introduced by external or internal sources). In the case of loss of containment due to pressure, the dent is re-formed under the increasing pressure and the gouge is propagated during the re-forming. Cracks developed on the shoulders of the dents can also be expected to propagate during the re-forming.

## 4.3 Stress Concentration Factors Due to Denting

Some information is available on the Stress Concentration Factors (SCF) that are associated with sharp shouldered denting (Fowler, 1991). The theoretical aspects of dent and gouge associated SCF have been studied by Svoboda, Gajdos (1994). This information indicates for longitudinal un-reformed dents the SCF is a function of the location around the circumference of the pipeline, the diameter to thickness ratio (D/t), and the depth of the dent relative to the pipe thickness or pipe diameter (H/t, H/D).

Fowler's results are summarized in Fig. 21 and 22 for the maximum SCF (located at the pipe crown – the point of maximum denting). Fowler's results are based on the results of extensive nonlinear finite element analysis studies. The study by Svoboda and Gajdos indicates that the SCF for denting is:

$$SCF = 1 + 6\, H/t$$

where H is the depth of the dent and t is the pipeline wall thickness. This relationship indicates SCF that are much greater than those developed by Fowler. Given the extensive nonlinear behavior found in the FEA studies, it is not unexpected that a linear elastic based SCF could be expected to over-predict the SCF.

As a result of study of the test data and results from analyses of flawed pipelines (Fowler, 1991; Miller, 1988) the following relationships were developed to evaluate the SCF associated with plain longitudinal denting without gouging (e.g. due to dropped objects) and the effects of the SCF on burst pressures.

Smooth denting and transverse denting ($H/R \leq 25\%$)

$$SCF_D = 1$$

Sharp longitudinal denting

$$SCF_D = (1 - H/R)^{-1}$$

$$SCF_D = 1 + 2\pi\, (H/R)^{0.5}$$

For dents associated with gouging (e.g. due to anchor dragging, jet sled damage) the following SCF was developed:

$$SCF_D = 1 + 0.2\, (H/t)^3$$

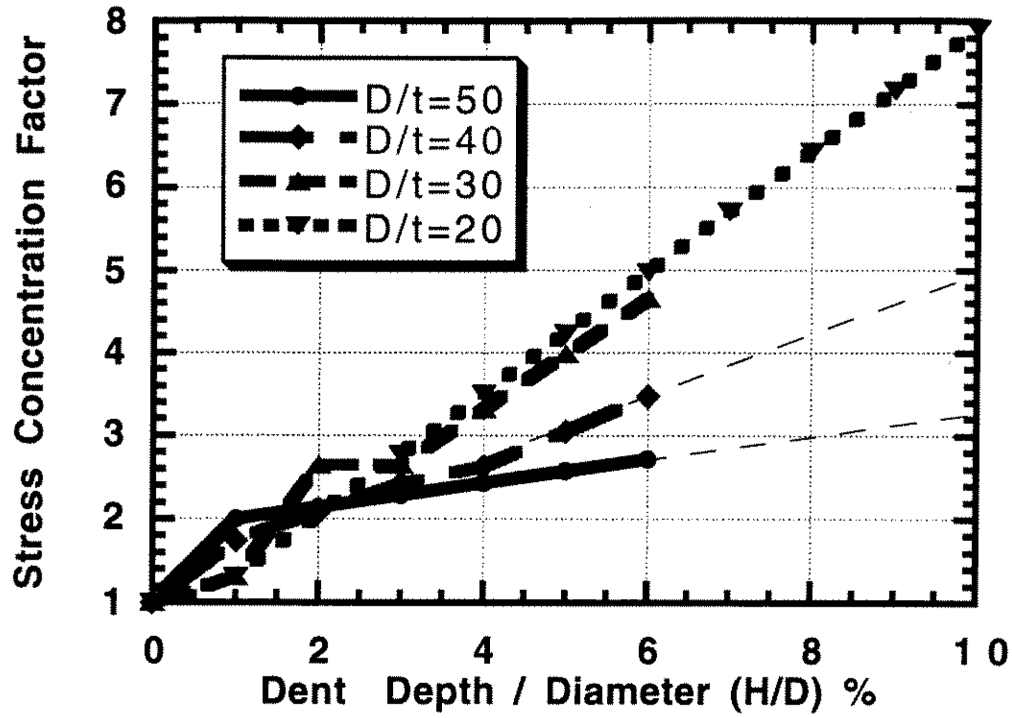


Fig. 21. Un-reformed longitudinal dent SCFs as function of dent depth normalized by the pipeline diameter

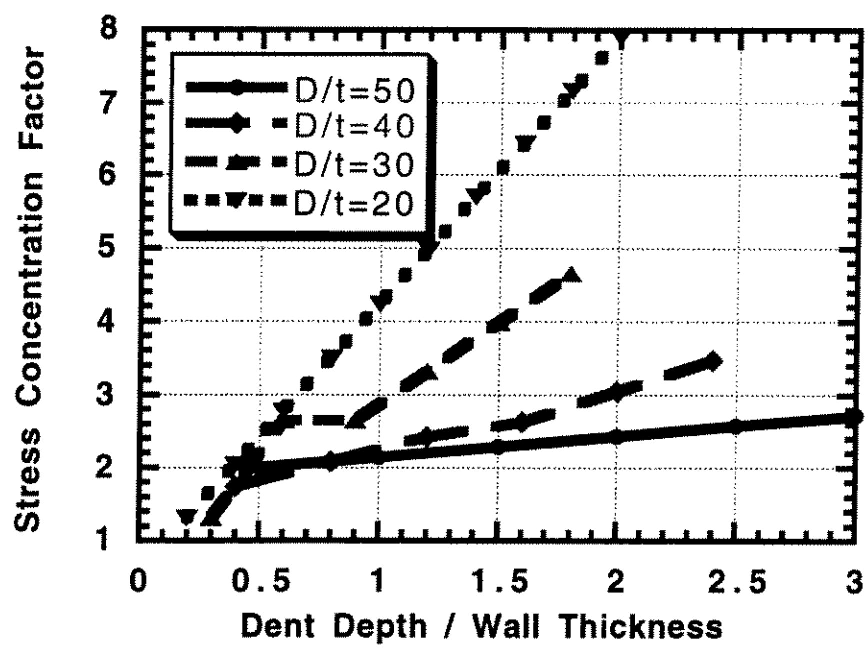


Fig. 22. Un-reformed longitudinal dent SCFs as function of dent depth normalized by the pipeline wall thickness

## 4.4 Stress Concentration Factors Due to Gouging

Extensive information is available on the SCF that are associated with gouging – cracking (Miller, 1988). All those reviewed during this study were based on elastic analysis methods. Figure 23 summarizes results from several of the analyses that were identified as being most appropriate for the denting – gouging SCF effects on pipeline burst pressure capacities. The two SCF relationships identified as *MisPSdeep* and *MisPS* shallow are those based on a Mises plane stress analysis of tensile induced cracking in which as the crack is developed bending stresses are introduced (Miller,1988).

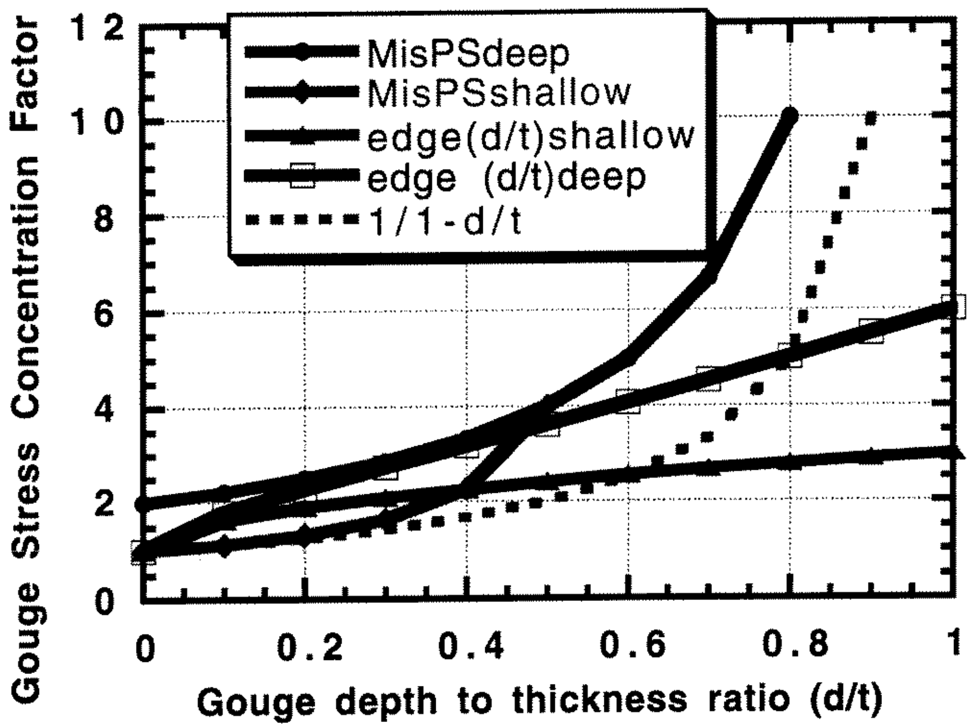


Fig. 23. Stress Concentration Factors due to gouging

The SCF relationship identified as 1/1-d/t (gouge depth, d, pipe thickness, t) is based on a plane stress Tresca and Mises, and plane strain Tresca analysis of cracking for pure tension (no bending stresses as cracking is developed). It is interesting to note that the crack root radius and flank angle (angle that describes the inclination of the sides of the crack) have no effect on this SCF. The SCF identified as edge shallow and deep is based on a tension loaded edge crack that has a root radius equal to the plate thickness. The deep relationship recognizes the increased tensile stress as the crack propagates through the plate thickness.

Based on an analysis of the applicability of these different analytical models, the relationship adopted in this study to define the SCF associated with plain gouging was:

$$SCF = (1 - de/t)^{-1}$$

This relationship does not take account of the interactions with denting; either during the denting process or during the dent re-forming under pressure process. To recognize these interactive effects, two contributions to the gouge – crack depth were identified:

- gouge – crack depth associated with denting = de
- propagation of gouge–crack depth associated with reforming the dent under pressure = dt

$$d = de + dt$$

The effective gouge depth is:

$$de = K\, d - dg$$

where K is the factor to recognize the mechanism used to introduce the gouging effect in extending the depth of the gouge below the gouge root. dg is introduced to enable recognition of the effect of grinding the gouge (a repair method).

The results provided by Hopkins (1990) in a study of the depth of cracking associated with the denting – gouging process when the pipeline is under pressure are summarized in Fig. 24. The data on maximum depth of cracking (determined using MPI) normalized by the pipeline wall thickness, a/t, associated with a gouge depth normalized by the pipeline wall thickness, d/t, is summarized in Fig. 24. It is apparent that there can be significant cracking developed below the root of the gouge during the denting – gouging process. K could range from 1.5 to 2.0.

If the gouge was introduced by a mechanical sawing or grinding process, K could be expected to be near unity. This indicates that the test data must be carefully regarded concerning how the gouge is introduced into the test specimens.

Propagation of the gouge under pressure reformation of the dent is difficult to determine. Initially, fracture mechanics was used to estimate how much the combined gouge – dent associated cracking might be propagated during the reformation of the dent (Barsom, Rolfe, 1987; Almar-Naess, 1985; Maxey, et al, 1971). The propagating stresses for the Type I stress conditions (tensile prying) developed stress intensity factors that generally fell in Region III or the rapidly propagating cracking region. These results indicated that the reforming cracking was most likely a ductile tearing mechanism rather than a cyclic strain – progressive cracking mechanism (Region II – moderate Stress Intensity Factor region) (Barson, Rolfe, 1987).

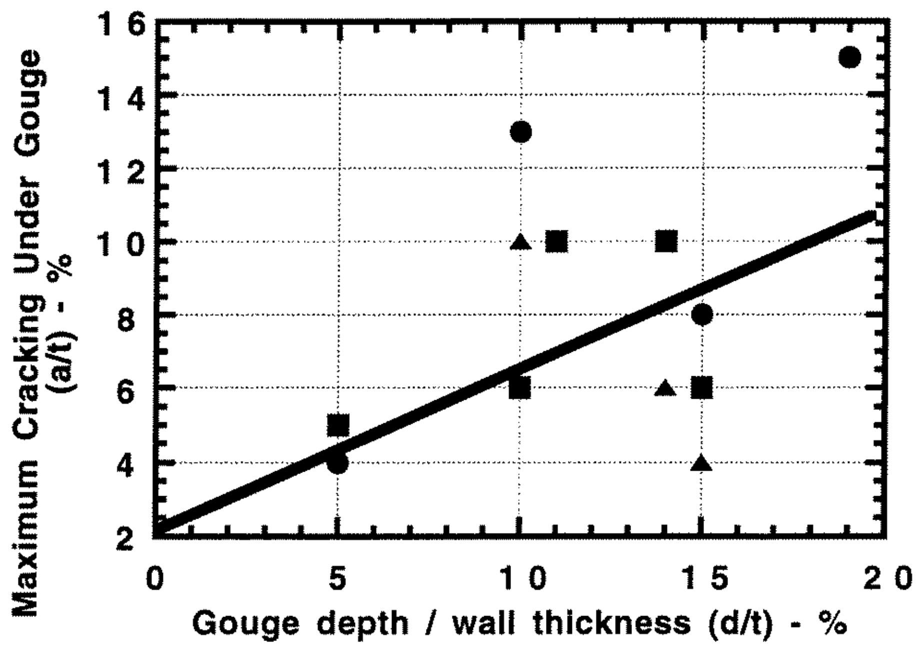


Fig. 24. Cracking developed below the gouge when the pipeline is dented and gouged under pressure

Given this insight, the crack propagation was related to the bending strains introduced during the pressure reformation process. The analysis indicated that the reformation bending strains could be expected to be a function of 16 times the dent depth to pipe radius (H/D):

$$\varepsilon_{rf} = 16\ H/D$$

These strains were evaluated to be responsible for the additional ductile tearing of the remaining gouged – dented cross section during pressure reforming:

$$dt = (16\ H/R)\ (t\text{-}de)$$

These studies resulted in two methods to evaluate the SCF associated with gouging and denting. The first method (Method 1) was based on separate SCF for the gouging and the dent reformation propagation:

$$SCF_G = (1 - d/t)^{-1}$$

$$SCF_D = 1 + 0.2\,(H/t)^3$$

$$SCF_{DG} = [(1 - d/t)^{-1}]\,[1 + 0.2\,(H/t)^3]$$

The second method (Method 2) was based on a single SCF that incorporated the gouge formation and propagation:

$$SCF_{DG} = \{[1 - (d/t) - [16\,H/D(1-d/t)]\}^{-1}$$

Analysis of Test Data, Figure 25 summarizes results from analysis of tests performed by British Gas Corporation (Jones, 1981) on 30-inch diameter X52 pipelines. The pipelines were first dented. The dent depths (H) to diameter ratios were in the range H/D = 1.0 % to 3.6 %.

A defect simulating a gouge was machined into the center of the dent parallel to the axis of the pipeline. The defects had depths (h) to wall thickness ratios that were h/t = 25%.

The analyses were based on the measured ultimate tensile strengths of the pipeline steel specimens (Suts). The reassessment damaged pipeline burst capacity was based on:

$$Pbd = (2\ Suts / SCF_{H,h})\,(t / D)$$

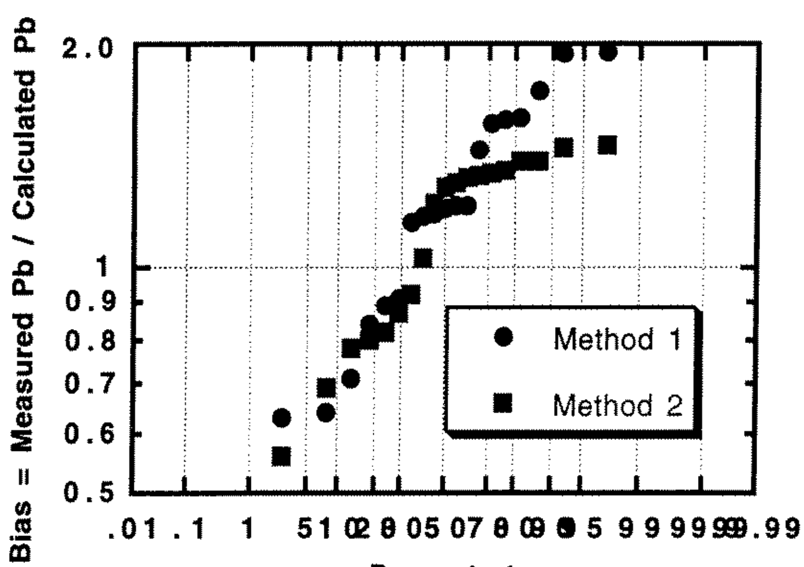


Fig. 25. British Gas Tests on 30-inch diameter pipelines with dents and gouges

Results of the analyses indicate Method 1 has $B_{50} = 1.2$ and $V_B = 33$ %. Method 2 has a $B_{50} = 1.3$ and $V_B = 25$ %. The bias was removed by introducing the specified minimum tensile stress of the pipeline steels in the reassessment formulation:

$$Pbd = (2\ SMTS / SCF_{H,h})\ (t / D)$$

Test data on dented and gouged pipelines were provided by Oberg, Rengard, and Wiik (1982). The first three tests involved only denting; the second three tests denting and gouging; and the last four tests denting, gouging, and grinding of the gouges (gouge depth and 0.2 to 1.5 mm beyond the gouge depth). These tests were published and analyzed by Song and Bai (1998). Song and Bai developed a modification of the Maxey - Kiefner – Battelle approach for determining the effects of longitudinal flaws on burst pressure capacities (Kiefner, et al, 1973). The modification utilized a Bilby-Cottrell-Swiden Dislocation Model, a modification for pipe steel toughness, and a Newman – Raju Stress Intensity Factor. The Song-Bai model did not account for the effects of denting. The test data indicate that longitudinal denting alone can have important effects on burst strength. Two identical pipeline specimens when dented, can develop very different burst capacities.

The combination of denting and gouging resulted in very significant reductions in the burst strength. Grinding the gouges improved the burst strength, however, there was still a significant effect of the gouging even though the gouges are removed by grinding and by over-grinding in an attempt to remove the cracks under the root of the gouges.

Table 3 includes an evaluation of the pipeline burst capacities based on the formulations developed during this project. The formulation for the dented pipeline results in reasonably unbiased results ($B_{50} = 0.95$). The formulation for the dented and gouged pipelines results in similarly unbiased results ($B_{50} = 1.0$). Based on the very limited test data, and the British Gas test data analysis discussed earlier, the COV of the Bias was estimated to be $V_B = 25$ %.

The dented – gouged – ground results are much more scattered. The analyses summarized in Table 3 were based on a crack depth below the gouge equal to K = 1.5 times the gouge depth. It is apparent that this resulted in an under-estimate of the crack depths below the gouge roots in three of the five cases.

Table 3. Dented – gouged pipeline test data analysis

| D mm | t | t/D | D/t | Suts | H/D | h/t | Pbm | PbND | SCF | SCF | SCF | SCF | Pb | Bias |
|---|---|---|---|---|---|---|---|---|---|---|---|---|---|---|
| Dented | mm | | | Mpa | | | Mpa | Mpa | c | H | d | t | DD | $B_{50}$ |
| 273 | 10 | 0.0366 | 27.32 | 630 | 0 | 0.000 | 46.0 | 46.12 | 1.00 | 1.000 | 1.00 | 1.00 | 46.1 | 1.00 |
| 273 | 10 | 0.0366 | 27.32 | 630 | 0.2 | 0.000 | 30.0 | 46.12 | 1.54 | 1.667 | 1.00 | 1.67 | 27.7 | 1.08 |
| 273 | 10 | 0.0366 | 27.32 | 630 | 0.2 | 0.000 | 21.2 | 46.12 | 2.18 | 1.667 | 1.00 | 1.67 | 27.7 | 0.77 |
| D/gouged | | | | | | | | | | | | | | |
| 814 | 20 | 0.0246 | 40.70 | 675 | 0.18 | 0.125 | 4.5 | 33.17 | 7.37 | 1.563 | 1.23 | 8.16 | 4.1 | 1.11 |
| 814 | 20 | 0.0246 | 40.70 | 675 | 0.12 | 0.125 | 7.4 | 33.17 | 4.48 | 1.316 | 1.23 | 4.01 | 8.3 | 0.90 |
| 814 | 20 | 0.0246 | 40.70 | 675 | 0.05 | 0.125 | 16.2 | 33.17 | 2.05 | 1.111 | 1.23 | 2.23 | 14.9 | 1.09 |
| D/G/ground | | | | | | | | | | | | | | |
| 814 | 20 | 0.0213 | 47.06 | 675 | 0.18 | 0.063 | 7.4 | 28.69 | 3.88 | 1.563 | 1.10 | 4.62 | 6.2 | 1.19 |
| 814 | 20 | 0.0206 | 48.54 | 675 | 0.18 | 0.028 | 27.0 | 27.81 | 1.03 | 1.563 | 1.04 | 3.72 | 7.5 | 3.61 |
| 814 | 20 | 0.0203 | 49.31 | 675 | 0.12 | 0.023 | 7.7 | 27.38 | 3.56 | 1.316 | 1.03 | 2.48 | 11.0 | 0.70 |
| 814 | 20 | 0.0203 | 49.33 | 675 | 0.12 | 0.013 | 6.8 | 27.36 | 4.02 | 1.316 | 1.02 | 2.39 | 11.4 | 0.59 |
| 814 | 20 | 0.0197 | 50.88 | 675 | 0.12 | 0.000 | 6.0 | 26.54 | 4.42 | 1.316 | 1.00 | 2.29 | 11.6 | 0.52 |

# 5 References


Almar-Naess, A. (Ed.) (1985). Fatigue Handbook, Offshore Steel Structures, Tapir Publishers, Trondheim, Norway.

American Society of Mechanical Engineers (ASME) (1993). Manual for Determining the Remaining Strength of Corroded Pipelines, Supplement to ANSI / ASME B31 Code for Pressure Piping, New York, NY.

Barson, J. M., and Rolfe, S. T. (1987). Fracture and Fatigue Control in Structures: Applications of Fracture Mechanics, Prentice-Hall, Inc., Englewood Cliffs, NJ.

Belonos, S. P., and Ryan, r. S. (1958). "Dents in Pipe," Oil and Gas Journal, Vol 10, Nov. 17, Houston, TX.

Bjorney, O.H., Cramer, E.H., and Sigurdson, G. (1997). "Probabilistic Calibrated Design Equation for Burst Strength Assessment of Corroded Pipes," Proceedings of the Seventh International Offshore and Polar Engineering Conference, International Society of Offshore and Polar Engineers, Golden, CO.

Collberg, L., Cramer, E. H., and Bjornoy, O. H. (1996). "Re-qualification of Pipeline Systems," Proceedings International Offshore and Polar Enigneering Conference, Intertnational Society of Offshore and Polar Enigneers, Golden, CO.



Collberg, L., Cramer, E. H., and Bjornoy, O. H. (1996). "Re-qualification of Pipeline Systems," Proceedings International Offshore and Polar Enigneering Conference, Intertnational Society of Offshore and Polar Enigneers, Golden, CO.



Det Norske Veritas (2000). *Corroded Pipelines, Recommended Practice RP-F101*, Hovik, Norway

Driver, R. G., and Zimmerman, T. J. E. (1998). "A Limit States Approach to the Design of Pipelines for Mechanical Damage," Proceedings Offshore Mechanics and Arctic Engineering Conference, Pipeline Symposium, American Society of Mechanical Engineers, New York.

Eiber, R., et al (1981). The Effects of Dents on the Failure Characteristics of Line Pipe, Battelle Columbus Report to AGA, NG-18, AGA Catalog No. L51403, Columbus, OH.

Fowler, J. R. (1991). "Criteria for Dent Acceptability in Offshore Pipelines," Proceedings of the Offshore Technology Conference, OTC 7311, Society of Petroleum Engineers, Richardson, TX.

Hopkins, P. (1990). A Full Scale Evaluation of the Behaviour of Dents and Defects in Linepipe for the European Pipeline Research Group, British Gas ERS Report R. 4516, British Gas Research & Technology, Newcastle upon Tyne, UK.

Hopkins, P., Jones, D. G., and Clyne, A. J. (1989). The Significance of dents in Transmission Pipelines, British Gas plc, Research & Technology, Engineering Research Station, Newcastle upon Tyne, UK.

Hopkins, P., and Jones, D. G (1992). "A Study of the Behavior of Long and Complex-Shaped Corrosion in transmission Pipelines," *Proceedings of the Offshore Mechanics and Arctic Engineering Conference*, Pipeline Symposium, American society of Mechanical Engineers, New York.

Jones, D. G. (1981). The Significance of Mechanical Damage in Pipelines, British Gas Corporation, Research & Technology, Engineering Research Station, Newcastle upon Tyne, UK.

Kiefner, J. F., et al (1989) "A Modified Criterion for Evaluating the Remaining Strength of Corroded Pipe, RSTRENG" Project PR 3-805 Pipeline Research Committee, American Gas Association, Houston, TX.

Kiefner, J. F., Maxey, W. A., Eiber, R. J., and Duffy, A. R. (1973). "Failure Stress Levels of Flaws in Pressurized Cylinders," Progress in Flaw Growth and Fracture Toughness Testing, ASTM STP 536, American Society for Testing and Materials, New York, NY.

Lara, L., Matias, J., Heredia, E., and Valle, O. (1998). *Transitory Criteria for Design and Evaluation of Submarine Pipelines in the Bay of Campeche*, First Meeting Report, Instituto Mexicano de Petroleo, Mexico, DF.

Maxey, W. A., et al. (1971). "Ductile Fracture Initiation, Propagation and Arrest in Cylindrical Vessels," Fracture Toughness, Proceedings National Symposium on Fracture Mechanics, ASTM STP 514, American Society for Testing and Materials, New York, NY.

Oberg, Tl., Rengard, O., and Wiik, T. (1982). Residual Strength of Dented Pipelines and Risers – Final Report, Technical Report to Joint Industry Project, Det Norske Veritas Report NO. 82-0567, Hovik, Norway.

Shannon, R. W. E. (1974). "The Failure Behaviour of Line Pipe Defects," International Journal of Pressure Vessels & Piping, Applied Science Publishers Ltd, UK.

Song, R., and Bai, Y. (1998). "Burst Reliability of Dented Pipes with Cracks," Proceedings of the Offshore and Polar Engineering Conference, American Society of Mechanical Engineers, New York, NY.

Stephens, D. R., Olson, R. J., and Rosenfeld, M. J. (1991). Topical Report on Pipeline Monitoring – Limit State Criteria, Report to Line Pipe Research Supervisory Committee, American Gas Association, Columbus, OH.

Svoboda, V., and Gajdos, L. (1994). "The Effect of Mechanical Damage on Gas-Pipeline Reliability," Proceedings Pipeline Risk Assessment, Rehabilitation and Repair Conference, Pipe Line Industry and Pipes & Pipelines International, Houston, TX.

Zimmerman, T. J. E., Cosham, A., Hopkins, P., and Sanderson, N. (1998). "Can Limit States Design be Used to Design a Pipeline Above 80% SMYS?" Proceedings Offshore Mechanics and Arctic Engineering Conference, Pipeline Symposium, American Society of Mechanical Engineers, New York.

# Appendix A – Corroded Pipeline Tests Burst Pressure Database

| No | Dia | t | SMYS | SMTS | Sig(y) | d | d/t | Pbm |
|---|---|---|---|---|---|---|---|---|
| | mm | mm | MPa | Mpa | MPa | mm | | Mpa |
| 1 | 762 | 9.398 | 358.50 | 471 | 404.80 | 3.708 | 0.395 | 11.19 |
| 2 | 762 | 9.398 | 358.50 | 471 | 404.80 | 3.708 | 0.395 | 11.17 |
| 3 | 762 | 9.398 | 358.50 | 471 | 404.80 | 3.988 | 0.424 | 11.72 |
| 4 | 762 | 9.525 | 358.50 | 471 | 440.00 | 6.096 | 0.640 | 11.52 |
| 5 | 762 | 9.525 | 358.50 | 471 | 405.50 | 5.309 | 0.557 | 10.52 |
| 6 | 609.60 | 9.271 | 241.30 | 350 | 279.30 | 6.883 | 0.742 | 7.59 |
| 7 | 609.60 | 9.271 | 241.30 | 350 | 279.30 | 6.375 | 0.688 | 8.03 |
| 8 | 609.60 | 9.271 | 241.30 | 350 | 279.30 | 6.375 | 0.688 | 8.41 |
| 9 | 609.60 | 9.398 | 241.30 | 350 | 288.30 | 6.629 | 0.705 | 7.17 |
| 10 | 609.60 | 9.525 | 241.30 | 350 | 288.30 | 7.163 | 0.752 | 8.03 |
| 11 | 609.60 | 9.27 | 241.30 | 350 | 288.30 | 6.629 | 0.715 | 7.03 |
| 12 | 609.60 | 9.271 | 241.30 | 350 | 288.30 | 5.563 | 0.600 | 8.38 |
| 13 | 609.60 | 9.271 | 241.30 | 350 | 288.30 | 5.842 | 0.630 | 9.10 |
| 14 | 609.60 | 9.271 | 241.30 | 350 | 288.30 | 6.629 | 0.715 | 9.10 |
| 15 | 609.60 | 9.652 | 241.30 | 350 | 288.30 | 6.375 | 0.660 | 9.21 |
| 16 | 609.60 | 9.398 | 241.30 | 350 | 288.30 | 4.775 | 0.508 | 9.31 |
| 17 | 609.60 | 9.398 | 241.30 | 350 | 288.30 | 6.096 | 0.649 | 9.48 |
| 18 | 609.60 | 9.525 | 241.30 | 350 | 288.30 | 6.096 | 0.640 | 9.92 |
| 19 | 609.60 | 9.271 | 241.30 | 350 | 288.30 | 6.629 | 0.715 | 10.00 |
| 20 | 609.60 | 9.525 | 241.30 | 350 | 288.30 | 6.375 | 0.669 | 8.28 |
| 21 | 609.60 | 9.525 | 241.30 | 350 | 288.30 | 7.417 | 0.779 | 10.28 |
| 22 | 609.60 | 9.525 | 241.30 | 350 | 288.30 | 5.563 | 0.584 | 10.48 |
| 23 | 609.60 | 9.525 | 241.30 | 350 | 288.30 | 4.775 | 0.501 | 10.48 |
| 24 | 609.60 | 9.525 | 241.30 | 350 | 288.30 | 4.496 | 0.472 | 10.48 |
| 25 | 609.60 | 9.652 | 241.30 | 350 | 288.30 | 6.883 | 0.713 | 10.41 |
| 26 | 762 | 9.525 | 358.50 | 471 | 427.60 | 9.525 | 1.000 | 12.03 |
| 27 | 762 | 9.525 | 358.50 | 471 | 422.80 | 3.708 | 0.389 | 12.69 |
| 28 | 762 | 9.525 | 358.50 | 471 | 427.60 | 2.921 | 0.307 | 13.07 |
| 29 | 762 | 9.525 | 358.50 | 471 | 456.60 | 5.842 | 0.613 | 12.24 |
| 30 | 762 | 9.525 | 358.50 | 471 | 486.90 | 5.309 | 0.557 | 14.76 |
| 31 | 762 | 9.525 | 358.5 | 471 | 458.6 | 5.309 | 0.557 | 13.79 |
| 32 | 508 | 8.255 | 241.3 | 350 | 282.8 | 5.309 | 0.643 | 7.93 |
| 33 | 508 | 8.255 | 241.3 | 350 | 283.4 | 5.563 | 0.674 | 11.69 |
| 34 | 406.4 | 7.874 | 172.4 | 264 | 197.2 | 5.842 | 0.742 | 7.59 |
| 35 | 406.4 | 7.874 | 172.4 | 264 | 197.2 | 6.096 | 0.774 | 8.76 |
| 36 | 406.4 | 7.874 | 172.4 | 264 | 197.2 | 7.163 | 0.910 | 5.66 |
| 37 | 406.4 | 7.874 | 172.4 | 264 | 197.2 | 6.909 | 0.877 | 6.14 |
| 38 | 406.4 | 7.874 | 172.4 | 264 | 195.9 | 5.055 | 0.642 | 8.90 |
| 39 | 609.6 | 10.59 | 241.3 | 350 | 346.2 | 7.366 | 0.696 | 9.62 |
| | | | | | | | | |

| No | Dia | t | SMYS | SMTS | Sig(y) | d | d/t | Pbm |
|---|---|---|---|---|---|---|---|---|
| | mm | mm | MPa | Mpa | MPa | mm | | Mpa |
| 40 | 609.6 | 10.41 | 241.3 | 350 | 322.8 | 9.652 | 0.927 | 11.45 |
| 41 | 609.6 | 10.06 | 241.3 | 350 | 346.2 | 9.144 | 0.909 | 6.41 |
| 42 | 609.6 | 11.28 | 241.3 | 350 | 346.2 | 5.588 | 0.495 | 13.10 |
| 43 | 609.6 | 9.296 | 241.3 | 350 | 371.7 | 6.985 | 0.751 | 10.10 |
| 44 | 609.6 | 9.246 | 241.3 | 350 | 358.6 | 6.452 | 0.698 | 8.72 |
| 45 | 609.6 | 9.017 | 241.3 | 350 | 358.6 | 7.341 | 0.814 | 10.38 |
| 46 | 609.6 | 8.103 | 241.3 | 350 | 327.6 | 5.486 | 0.677 | 11.94 |
| 47 | 609.6 | 8.433 | 241.3 | 350 | 310.3 | 5.588 | 0.663 | 12.08 |
| 48 | 609.6 | 9.525 | 241.3 | 350 | 371 | 7.493 | 0.787 | 5.12 |
| 49 | 609.6 | 9.525 | 255.1 | 366 | 336.6 | 8.128 | 0.853 | 5.43 |
| 50 | 508 | 7.925 | 241.3 | 350 | 344.8 | 6.401 | 0.808 | 4.92 |
| 51 | 508 | 7.747 | 241.3 | 350 | 380 | 5.334 | 0.689 | 11.54 |
| 52 | 609.6 | 9.169 | 241.3 | 350 | 326.9 | 8.103 | 0.884 | 8.90 |
| 53 | 609.6 | 9.169 | 241.3 | 350 | 284.1 | 7.239 | 0.790 | 10.17 |
| 54 | 609.6 | 9.017 | 241.3 | 350 | 346.9 | 6.172 | 0.684 | 12.01 |
| 55 | 609.6 | 9.423 | 241.3 | 350 | 310.3 | 7.01 | 0.744 | 9.36 |
| 56 | 609.6 | 9.423 | 241.3 | 350 | 310.3 | 7.391 | 0.784 | 9.36 |
| 57 | 609.6 | 9.449 | 241.3 | 350 | 332.4 | 7.214 | 0.763 | 11.03 |
| 58 | 609.6 | 9.246 | 241.3 | 350 | 331.7 | 5.69 | 0.615 | 11.34 |
| 59 | 609.6 | 9.296 | 241.3 | 350 | 296.6 | 6.147 | 0.661 | 12.47 |
| 60 | 609.6 | 9.296 | 241.3 | 350 | 355.2 | 4.851 | 0.522 | 10.92 |
| 61 | 609.6 | 9.347 | 241.3 | 350 | 329 | 7.315 | 0.783 | 10.55 |
| 62 | 508 | 7.188 | 241.3 | 350 | 261.4 | 4.623 | 0.643 | 7.52 |
| 63 | 508 | 6.960 | 241.3 | 350 | 279.3 | 3.302 | 0.474 | 11.99 |
| 64 | 508 | 7.899 | 241.3 | 350 | 243.4 | 6.071 | 0.769 | 11.68 |
| 65 | 508 | 7.899 | 241.3 | 350 | 243.4 | 2.667 | 0.338 | 11.68 |
| 66 | 508 | 6.756 | 241.3 | 350 | 277.2 | 3.658 | 0.541 | 10.39 |
| 67 | 508 | 7.849 | 241.3 | 350 | 289 | 5.537 | 0.705 | 12.52 |
| 68 | 762 | 9.449 | 358.5 | 471 | 418.6 | 3.302 | 0.349 | 12.72 |
| 69 | 762 | 9.550 | 358.5 | 471 | 358.6 | 5.842 | 0.612 | 10.45 |
| 70 | 762 | 9.525 | 358.5 | 471 | 415.9 | 3.556 | 0.373 | 12.52 |
| 71 | 762 | 9.703 | 358.5 | 471 | 437.9 | 3.683 | 0.380 | 13.12 |
| 72 | 762 | 9.550 | 358.5 | 471 | 406.9 | 3.302 | 0.346 | 12.31 |
| 73 | 762 | 9.601 | 358.5 | 471 | 428.3 | 2.794 | 0.291 | 13.21 |
| 74 | 762 | 9.627 | 358.5 | 471 | 451 | 4.318 | 0.449 | 12.24 |
| 75 | 762 | 9.677 | 358.5 | 471 | 358.6 | 7.62 | 0.787 | 7.72 |
| 76 | 762 | 9.601 | 358.5 | 471 | 422.1 | 4.318 | 0.450 | 11.86 |
| 77 | 762 | 9.576 | 358.5 | 471 | 426.2 | 4.064 | 0.424 | 12.34 |
| 78 | 762 | 9.474 | 359.5 | 471 | 415.2 | 2.794 | 0.295 | 12.69 |
| 79 | 609.6 | 9.525 | 255.1 | 366 | 289.7 | 8.179 | 0.859 | 5.55 |

| No | Dia | t | SMYS | SMTS | Sig(y) | d | d/t | Pbm |
|---|---|---|---|---|---|---|---|---|
| | mm | mm | MPa | Mpa | MPa | mm | | Mpa |
| 80 | 762 | 9.271 | 358.5 | 471 | 404.1 | 5.817 | 0.627 | 6.81 |
| 81 | 762 | 9.525 | 358.5 | 471 | 474.5 | 6.223 | 0.653 | 6.84 |
| 82 | 762 | 9.525 | 386.1 | 471 | 444.1 | 3.81 | 0.400 | 13.59 |
| 83 | 508 | 6.604 | 358.5 | 471 | 420.7 | 5.537 | 0.838 | 5.76 |
| 84 | 914.4 | 8.382 | 448.2 | 495 | 448.3 | 5.537 | 0.661 | 5.35 |
| 85 | 762 | 7.569 | 413.7 | 471 | 489.7 | 6.833 | 0.903 | 5.62 |
| 86 | 558.8 | 5.029 | 358.5 | 542 | 420.7 | 3.759 | 0.747 | 5.71 |
| 87 | 508 | 6.35 | 413.7 | 517 | | 2.54 | 0.400 | 14.55 |
| 88 | 508 | 6.35 | 413.7 | 471 | | 2.54 | 0.400 | 13.85 |
| 89 | 508 | 6.35 | 413.7 | 517 | | 2.54 | 0.400 | 12.35 |
| 90 | 508 | 6.35 | 413.7 | 517 | | 2.54 | 0.400 | 15.85 |
| 91 | 508 | 6.35 | 413.7 | 517 | | 2.54 | 0.400 | 11.25 |
| 92 | 508 | 6.35 | 413.7 | 517 | | 2.54 | 0.400 | 11.55 |
| 93 | 508 | 6.35 | 413.7 | 517 | | 2.54 | 0.400 | 13.05 |
| 94 | 508 | 6.35 | 413.7 | 517 | | 0 | 0.000 | 13.05 |
| 95 | 508 | 6.35 | 413.7 | 517 | | 0 | 0.000 | 13.05 |
| 96 | 508 | 6.35 | 413.7 | 517 | | 2.54 | 0.400 | 15.25 |
| 97 | 508 | 6.35 | 413.7 | 517 | | 2.54 | 0.400 | 11.05 |
| 98 | 508 | 6.35 | 413.7 | 517 | | 2.54 | 0.400 | 10.55 |
| 99 | 508 | 6.36 | 413.7 | 517 | | 0 | 0.000 | 15.45 |
| 100 | 508 | 6.4 | 413.7 | 517 | | 0 | 0.000 | 15.25 |
| 101 | 508 | 6.4 | 413.7 | 517 | | 3.429 | 0.536 | 8.00 |
| 102 | 508 | 6.4 | 413.7 | 517 | | 2.159 | 0.337 | 11.80 |
| 103 | 508 | 6.4 | 413.7 | 517 | | 3.008 | 0.470 | 12.50 |
| 104 | 508 | 6.4 | 413.7 | 517 | | 2.944 | 0.460 | 9.80 |
| 105 | 508 | 6.4 | 413.7 | 517 | | 3.366 | 0.526 | 8.45 |
| 106 | 508 | 6.4 | 413.7 | 517 | | 3.175 | 0.496 | 8.40 |
| 107 | 610 | 12.34 | 358.5 | 471 | 451 | 4.936 | 0.400 | 14.44 |
| 108 | 610 | 12.34 | 358.5 | 471 | 447 | 4.936 | 0.400 | 14.00 |
| 109 | 610 | 12.34 | 358.5 | 471 | 447 | 4.936 | 0.400 | 15.45 |
| 110 | 610 | 12.34 | 358.5 | 471 | 447 | 4.936 | 0.400 | 16.46 |
| 111 | 610 | 12.34 | 358.5 | 471 | 447 | 4.936 | 0.400 | 18.45 |
| 112 | 610 | 12.34 | 358.5 | 471 | 451 | 0 | 0.000 | 21.30 |
| 113 | 610 | 12.34 | 358.5 | 471 | 451 | 4.936 | 0.400 | 14.90 |
| 114 | 610 | 12.34 | 358.5 | 471 | 451 | 0 | 0.000 | 21.20 |
| 115 | 610 | 12.34 | 358.5 | 471 | 451 | 4.936 | 0.400 | 14.40 |
| 116 | 914 | 22 | 413.7 | 517 | 434 | 0 | 0.000 | 26.30 |
| 117 | 914 | 22 | 413.7 | 517 | 434 | 0 | 0.000 | 26.40 |
| 118 | 914 | 22 | 413.7 | 517 | 434 | 6.6 | 0.300 | 18.70 |
| 119 | 914 | 22 | 413.7 | 517 | 434 | 6.16 | 0.280 | 19.50 |

| No | Dia | t | SMYS | SMTS | Sig(y) | d | d/t | Pbm |
|---|---|---|---|---|---|---|---|---|
| | mm | mm | MPa | Mpa | MPa | mm | | Mpa |
| 120 | 914 | 22 | 413.7 | 517 | 434 | 10.34 | 0.470 | 14.70 |
| 121 | 914 | 22 | 413.7 | 517 | 434 | 11 | 0.500 | 13.00 |
| 122 | 914 | 22 | 413.7 | 517 | 434 | 15.18 | 0.690 | 8.60 |
| 123 | 914 | 22 | 413.7 | 517 | 434 | 14.74 | 0.670 | 8.10 |
| 124 | 914 | 22 | 413.7 | 517 | 434 | 14.74 | 0.670 | 8.20 |
| 125 | 324 | 5.93 | 317.2 | 432 | 378 | 4.685 | 0.790 | 13.49 |
| 126 | 324 | 6.07 | 317.2 | 432 | 381 | 4.006 | 0.660 | 14.29 |
| 127 | 324 | 5.84 | 317.2 | 432 | 382 | 3.913 | 0.670 | 16.29 |
| 128 | 324 | 5.99 | 317.2 | 432 | 351 | 4.672 | 0.780 | 15.36 |
| 129 | 324 | 6.00 | 317.2 | 432 | 403 | 4.38 | 0.730 | 16.09 |
| 130 | 324 | 6.07 | 317.2 | 432 | 421 | 2.914 | 0.480 | 16.95 |
| 131 | 324 | 5.58 | 317.2 | 432 | 346 | 4.408 | 0.790 | 13.00 |
| 132 | 324 | 6.14 | 317.2 | 432 | 375 | 2.395 | 0.390 | 15.78 |
| 133 | 324 | 6.16 | 317.2 | 432 | 356 | 4.497 | 0.730 | 14.29 |
| 134 | 324 | 5.95 | 317.2 | 432 | 356 | 4.165 | 0.700 | 15.57 |
| 135 | 324 | 6.02 | 317.2 | 432 | 359 | 1.987 | 0.330 | 16.12 |
| 136 | 324 | 6.40 | 317.2 | 432 | 382 | 3.23 | 0.505 | 16.64 |
| 137 | 324 | 6.01 | 317.2 | 432 | 382 | 3.6 | 0.599 | 16.22 |
| 138 | 324 | 6.30 | 317.2 | 432 | 373 | 3.57 | 0.567 | 15.95 |
| 139 | 323 | 6.31 | 317.2 | 432 | 373 | 3.73 | 0.591 | 14.16 |
| 140 | 324 | 6.16 | 317.2 | 432 | 356 | 3.73 | 0.606 | 18.85 |
| 141 | 324 | 6.27 | 317.2 | 432 | 356 | 3.76 | 0.600 | 19.13 |
| 142 | 324 | 6.25 | 317.2 | 432 | 356 | 3.79 | 0.606 | 19.27 |
| 143 | 324 | 6.18 | 317.2 | 432 | 421 | 3.75 | 0.607 | 19.44 |
| 144 | 325 | 6.45 | 317.2 | 432 | 373 | 3.05 | 0.473 | 15.81 |
| 145 | 324 | 6.40 | 317.2 | 432 | 373 | 3.72 | 0.581 | 13.87 |
| 146 | 325 | 6.45 | 317.2 | 432 | 356 | 3.79 | 0.588 | 14.84 |
| 147 | 324 | 6.35 | 317.2 | 432 | 356 | 3.72 | 0.586 | 15.53 |
| 148 | 322 | 6.27 | 317.2 | 432 | 381 | 3.77 | 0.601 | 17.61 |
| 149 | 324 | 6.29 | 317.2 | 432 | 378 | 3.79 | 0.603 | 15.11 |
| 150 | 324 | 6.24 | 317.2 | 432 | 381 | 3.79 | 0.607 | 15.67 |
| 151 | 324 | 6.16 | 317.2 | 432 | 378 | 3.70 | 0.601 | 15.25 |

# Appendix B – Dented - Gouged Pipeline Tests Burst Pressure Database

| Spec. No. | D (in) | t (in) | D/t | sy (ksi) | sf(ksi) | DD(in) | d(in) |
|---|---|---|---|---|---|---|---|
| BGC-1 | 12.75 | 0.26 | 49.0 | 57.0 | 59.2 | *0.25* | *0.026* |
| BGC-2 | 12.75 | 0.27 | 46.8 | 57.0 | 56.1 | 0.28 | 0.030 |
| BGC-3 | 12.75 | 0.29 | 43.6 | 57.0 | 58.0 | 0.23 | 0.038 |
| BGC-4 | 12.75 | 0.30 | 43.2 | 57.0 | 14.3 | 0.62 | 0.059 |
| BGC-5 | 12.75 | 0.30 | 43.2 | 57.0 | 11.8 | 0.63 | 0.059 |
| BGC-6 | 12.75 | 0.31 | 41.6 | 57.0 | 16.7 | 0.69 | 0.049 |
| BGC-7 | 12.75 | 0.30 | 42.0 | 57.0 | 6.4 | 0.98 | 0.091 |
| BGC-8 | 12.75 | 0.30 | 42.5 | 57.0 | 7.0 | 1.02 | 0.084 |
| BGC-9 | 12.75 | 0.27 | 47.3 | 57.0 | 9.0 | 0.93 | 0.089 |
| BGC-10 | 18.00 | 0.32 | 55.6 | 50.5 | 35.9 | 0.17 | 0.110 |
| BGC-11 | 18.00 | 0.31 | 57.3 | 50.5 | 39.0 | 0.08 | 0.110 |
| BGC-12 | 18.00 | 0.32 | 55.6 | 50.5 | 44.4 | 0.09 | 0.110 |
| BGC-13 | 18.00 | 0.32 | 56.5 | 50.5 | 54.5 | 0.37 | 0.051 |
| BGC-14 | 18.00 | 0.31 | 57.4 | 50.5 | 53.7 | 0.36 | 0.047 |
| BGC-15 | 18.00 | 0.31 | 57.4 | 50.5 | 53.4 | 0.37 | 0.047 |
| BGC-16 | 18.00 | 0.32 | 56.6 | 50.5 | 45.0 | 1.08 | 0.035 |
| BGC-17 | 18.00 | 0.30 | 60.0 | 50.5 | 51.5 | 1.08 | 0.030 |
| BGC-18 | 18.00 | 0.31 | 57.9 | 50.5 | 53.9 | 1.08 | 0.028 |
| BGC-19 | 24.00 | 0.47 | 51.2 | 50.5 | 6.4 | 1.68 | 0.072 |
| BGC-20 | 24.00 | 0.47 | 51.2 | 50.5 | 7.7 | 1.75 | 0.062 |
| BGC-21 | 24.00 | 0.47 | 51.2 | 50.5 | 9.5 | 1.58 | 0.068 |
| BGC-22 | 24.00 | 0.47 | 51.2 | 50.5 | 15.9 | 1.58 | 0.074 |
| BGC-23 | 24.00 | 0.47 | 51.2 | 50.5 | 8.3 | 1.78 | 0.103 |
| BGC-24 | 24.00 | 0.47 | 51.2 | 50.5 | 26.4 | 1.10 | 0.051 |
| BGC-25 | 24.00 | 0.47 | 51.2 | 50.5 | 13.0 | 1.13 | 0.060 |
| BGC-26 | 24.00 | 0.47 | 51.2 | 50.5 | 16.0 | 1.10 | 0.052 |
| BGC-27 | 24.00 | 0.47 | 51.2 | 50.5 | 32.8 | 1.20 | 0.046 |
| BGC-28 | 24.00 | 0.47 | 51.2 | 50.5 | 33.0 | 1.22 | 0.049 |
| BGC-29 | 24.00 | 0.47 | 51.2 | 50.5 | 26.6 | 0.60 | 0.133 |
| BGC-30 | 24.00 | 0.47 | 51.2 | 50.5 | 17.8 | 0.67 | 0.176 |
| BGC-31 | 24.00 | 0.47 | 51.2 | 50.5 | 15.9 | 0.62 | 0.135 |
| BGC-32 | 24.00 | 0.47 | 51.2 | 50.5 | 28.7 | 0.55 | 0.125 |
| BGC-33 | 30.00 | 0.47 | 64.0 | 50.5 | 17.0 | 1.11 | 0.084 |
| BGC-34 | 30.00 | 0.47 | 64.0 | 50.5 | 16.5 | 1.05 | 0.089 |
| BGC-35 | 30.00 | 0.47 | 64.0 | 50.5 | 23.5 | 1.02 | 0.098 |
| BGC-36 | 30.00 | 0.47 | 64.0 | 50.5 | 24.7 | 0.93 | 0.098 |
| BGC-37 | 42.00 | 0.56 | 74.7 | 50.5 | 23.5 | 2.01 | 0.120 |
| BGC-38 | 42.00 | 0.56 | 74.7 | 50.5 | 24.3 | 1.87 | 0.130 |
| BGC-39 | 42.00 | 0.56 | 74.7 | 50.5 | 24.7 | 1.96 | 0.116 |
| BGC-40 | 42.00 | 0.56 | 74.7 | 50.5 | 19.4 | 3.02 | 0.065 |
| BGC-41 | 42.00 | 0.56 | 74.7 | 50.5 | 24.7 | 3.06 | 0.063 |
| BGC-42 | 30.00 | 0.47 | 64.0 | 60.0 | 14.1 | 0.92 | 0.109 |

| Spec. No. | D (in) | t (in) | D/t | sy (ksi) | sf(ksi) | DD(in) | d(in) |
|---|---|---|---|---|---|---|---|
| BGC-43 | 30.00 | 0.47 | 64.0 | 60.0 | 5.5 | 1.41 | 0.109 |
| BGC-44 | 30.00 | 0.47 | 64.0 | 60.0 | 26.1 | 0.35 | 0.109 |
| BGC-45 | 30.00 | 0.47 | 64.0 | 60.0 | 18.5 | 0.53 | 0.109 |
| BGC-46 | 30.00 | 0.47 | 64.0 | 60.0 | 10.2 | 1.09 | 0.135 |
| BGC-47 | 30.00 | 0.47 | 64.0 | 60.0 | 4.7 | 1.81 | 0.135 |
| BGC-48 | 30.00 | 0.47 | 64.0 | 60.0 | 11.5 | 0.98 | 0.135 |
| BGC-49 | 30.00 | 0.47 | 64.0 | 60.0 | 23.4 | 0.62 | 0.135 |
| BGC-50 | 30.00 | 0.47 | 64.0 | 60.0 | 4.3 | 2.09 | 0.135 |
| BGC-51 | 30.00 | 0.47 | 64.0 | 60.0 | 22.2 | 0.38 | 0.135 |
| *BGC-52* | 30.00 | 0.47 | 64.0 | 60.0 | 17.0 | 0.50 | 0.116 |
| BGC-53 | 30.00 | 0.47 | 64.0 | 60.0 | 14.7 | 0.54 | 0.116 |
| BGC-54 | 30.00 | 0.47 | 64.0 | 60.0 | 18.3 | 0.49 | 0.116 |
| BGC-55 | 30.00 | 0.47 | 64.0 | 60.0 | 18.8 | 0.44 | 0.116 |
| BGC-56 | 30.00 | 0.47 | 64.0 | 60.0 | 11.4 | 0.56 | 0.116 |
| BGC-57 | 30.00 | 0.47 | 64.0 | 60.0 | 34.2 | 0.38 | 0.175 |
| BGC-58 | 30.00 | 0.47 | 64.0 | 60.0 | 31.0 | 0.49 | 0.175 |
| BGC-59 | 30.00 | 0.47 | 64.0 | 60.0 | 27.9 | 0.57 | 0.175 |
| BGC-60 | 30.00 | 0.47 | 64.0 | 60.0 | 35.6 | 0.42 | 0.175 |
| BGC-61 | 30.00 | 0.47 | 64.0 | 60.0 | 32.2 | 0.48 | 0.175 |
| BGC-62 | 30.00 | 0.47 | 64.0 | 60.0 | 87.0 | 0.73 | 0.026 |
| BGC-63 | 30.00 | 0.47 | 64.0 | 60.0 | 67.2 | 0.61 | 0.040 |
| BGC-64 | 30.00 | 0.47 | 64.0 | 60.0 | 61.2 | 0.71 | 0.045 |
| BGC-65 | 30.00 | 0.47 | 64.0 | 60.0 | 59.8 | 0.75 | 0.052 |
| BGC-66 | 30.00 | 0.47 | 64.0 | 60.0 | 58.1 | 0.73 | 0.049 |
| BGC-67 | 30.00 | 0.47 | 64.0 | 60.0 | 56.7 | 0.73 | 0.100 |
| BGC-68 | 30.00 | 0.47 | 64.0 | 60.0 | 56.4 | 0.76 | 0.045 |
| BGC-69 | 30.00 | 0.47 | 64.0 | 60.0 | 20.2 | 0.81 | 0.020 |
| BGC-70 | 30.00 | 0.47 | 64.0 | 60.0 | 15.1 | 2.07 | 0.094 |
| BGC-71 | 30.00 | 0.47 | 64.0 | 60.0 | 28.5 | 2.09 | 0.010 |
| BGC-72 | 30.00 | 0.47 | 64.0 | 60.0 | 10.6 | 2.09 | 0.011 |
| BGC-73 | 30.00 | 0.47 | 64.0 | 60.0 | 29.8 | 2.29 | 0.007 |
| BGC-74 | 30.00 | 0.47 | 64.0 | 60.0 | 42.4 | 2.30 | 0.117 |
| BGC-75 | 30.00 | 0.47 | 64.0 | 60.0 | 36.6 | 2.65 | 0.117 |
| BGC-76 | 30.00 | 0.47 | 64.0 | 52.0 | 57.4 | 0.45 | 0.117 |
| BGC-77 | 30.00 | 0.47 | 64.0 | 52.0 | 55.6 | 0.60 | 0.117 |
| BGC-78 | 30.00 | 0.47 | 64.0 | 52.0 | 53.3 | 0.72 | 0.117 |
| BGC-79 | 30.00 | 0.47 | 64.0 | 52.0 | 52.7 | 0.78 | 0.117 |
| BGC-80 | 30.00 | 0.47 | 64.0 | 52.0 | 44.0 | 0.99 | 0.117 |
| BGC-81 | 30.00 | 0.47 | 64.0 | 52.0 | 54.1 | 0.50 | 0.117 |
| BGC-82 | 30.00 | 0.47 | 64.0 | 52.0 | 45.4 | 0.81 | 0.117 |
| BGC-83 | 30.00 | 0.47 | 64.0 | 52.0 | 43.7 | 0.66 | 0.117 |
| BGC-84 | 30.00 | 0.47 | 64.0 | 52.0 | 42.7 | 0.72 | 0.117 |
| BGC-85 | 30.00 | 0.47 | 64.0 | 52.0 | 41.6 | 0.78 | 0.117 |
| BGC-86 | 30.00 | 0.47 | 64.0 | 52.0 | 40.5 | 0.93 | 0.117 |

| Spec. No. | D (in) | t (in) | D/t | sy (ksi) | sf(ksi) | DD(in) | d(in) |
|---|---|---|---|---|---|---|---|
| BGC-87 | 30.00 | 0.47 | 64.0 | 52.0 | 38.3 | 1.06 | 0.117 |
| BGC-88 | 30.00 | 0.47 | 64.0 | 52.0 | 42.8 | 0.46 | 0.117 |
| BGC-89 | 30.00 | 0.47 | 64.0 | 52.0 | 39.0 | 0.61 | 0.117 |
| BGC-90 | 30.00 | 0.47 | 64.0 | 52.0 | 38.4 | 0.43 | 0.117 |
| BGC-91 | 30.00 | 0.47 | 64.0 | 52.0 | 37.8 | 0.58 | 0.117 |
| BGC-92 | 30.00 | 0.47 | 64.0 | 52.0 | 33.1 | 0.74 | 0.117 |
| BGC-93 | 30.00 | 0.47 | 64.0 | 52.0 | 34.0 | 0.85 | 0.117 |
| BGC-94 | 30.00 | 0.47 | 64.0 | 52.0 | 28.9 | 1.22 | 0.117 |
| BGC-95 | 30.00 | 0.47 | 64.0 | 52.0 | 27.2 | 0.99 | 0.117 |
| BGC-96 | 30.00 | 0.47 | 64.0 | 52.0 | 26.7 | 1.19 | 0.117 |
| BGC-97 | 30.00 | 0.47 | 64.0 | 52.0 | 21.7 | 1.34 | 0.117 |
| BGC-98 | 30.00 | 0.47 | 64.0 | 52.0 | 18.4 | 1.61 | 0.117 |
| BGC-99 | 30.00 | 0.47 | 64.0 | 52.0 | 64.5 | 0.41 | 0.122 |
| BGC-100 | 30.00 | 0.47 | 64.0 | 52.0 | 66.4 | 0.39 | 0.122 |
| BGC-101 | 30.00 | 0.47 | 64.0 | 52.0 | 65.8 | 0.40 | 0.125 |
| BGC-102 | 30.00 | 0.47 | 64.0 | 52.0 | 53.4 | 0.76 | 0.129 |
| BGC-103 | 30.00 | 0.47 | 64.0 | 52.0 | 50.0 | 0.78 | 0.129 |
| BGC-104 | 30.00 | 0.47 | 64.0 | 52.0 | 47.3 | 0.83 | 0.123 |
| BGC-105 | 30.00 | 0.47 | 64.0 | 52.0 | 44.8 | 0.89 | 0.130 |
| BGC-106 | 30.00 | 0.47 | 64.0 | 52.0 | 34.3 | 1.09 | 0.128 |
| BGC-107 | 30.00 | 0.47 | 64.0 | 52.0 | 20.9 | 1.20 | 0.123 |
| BGC-108 | 30.00 | 0.47 | 64.0 | 52.0 | 56.8 | 0.57 | 0.117 |
| BGC-109 | 30.00 | 0.47 | 64.0 | 52.0 | 51.5 | 0.64 | 0.117 |
| BGC-110 | 30.00 | 0.47 | 64.0 | 52.0 | 45.0 | 0.96 | 0.117 |
| BGC-111 | 30.00 | 0.47 | 64.0 | 52.0 | 40.1 | 0.41 | 0.117 |
| BGC-112 | 30.00 | 0.47 | 64.0 | 52.0 | 20.9 | 0.78 | 0.117 |
| BGC-113 | 30.00 | 0.47 | 64.0 | 52.0 | 55.2 | 0.30 | 0.117 |
| BGC-114 | 30.00 | 0.47 | 64.0 | 52.0 | 35.9 | 0.70 | 0.117 |
| BGC-115 | 30.00 | 0.47 | 64.0 | 52.0 | 32.0 | 0.52 | 0.117 |
| BGC-116 | 30.00 | 0.47 | 64.0 | 52.0 | 30.2 | 0.75 | 0.117 |
| BGC-117 | 30.00 | 0.47 | 64.0 | 52.0 | 22.3 | 1.08 | 0.117 |
| DTZ/1P | 30.00 | 0.50 | 60.0 | 62.4 | 20.0 | 0.46 | 0.240 |
| DTZ/2P | 30.00 | 0.50 | 60.0 | 62.4 | 11.7 | 0.98 | 0.138 |
| DTZ/1R | 30.00 | 0.50 | 60.0 | 62.4 | 23.4 | 1.05 | 0.103 |
| DTZ/2R | 30.00 | 0.50 | 60.0 | 62.4 | 20.7 | 1.06 | 0.095 |